行政院國家科學委員會專題研究計畫　期中進度報告

超寬頻無線通訊系統在智慧型天線通道上之性能研究(2/3)

計畫類別：個別型計畫
計畫編號：NSC94-2213-E-009-030-
執行期間：94 年 08 月 01 日至 95 年 07 月 31 日
執行單位：國立交通大學電信工程學系(所)

計畫主持人：王蒞君

報告類型：精簡報告
報告附件：出席國際會議研究心得報告及發表論文
處理方式：本計畫可公開查詢

中　華　民　國 95 年 5 月 3 日

行政院國家科學委員會補助專題研究計畫期中進度報告

超寬頻無線通訊系統在智慧型天線通道上之性能研究

計畫類別：個別型計畫
計畫編號：NSC 94-2213-E-009-030
執行期間：94 年 8 月 1 日至 95 年 7 月 31 日

計畫主持人：王蒞君 教授
共同主持人：
計畫參與人員：劉維正

成果報告類型(依經費核定清單規定繳交)：精簡報告

本成果報告包括以下應繳交之附件：
□赴國外出差或研習心得報告一份
□赴大陸地區出差或研習心得報告一份
□出席國際學術會議心得報告及發表之論文各一份
□國際合作研究計畫國外研究報告書一份

處理方式：除產學合作研究計畫、提升產業技術及人才培育研究計畫、列管計畫及下列情形者外，得立即公開查詢
□涉及專利或其他智慧財產權，□一年☑二年後可公開查詢

執行單位：國立交通大學電信工程學系

中　　華　　民　　國 95 年 5 月 3 日

摘要

本年度的研究計劃之研究成果可分為兩大部份：

一、在具有隨機群集及射線特性的高度頻率選擇性衰減通道下以脈波為基礎之超寬頻系統效能分析

在這一部份我們推導出在 IEEE 802.15.3a 通道下，二元信號的位元錯誤率。雖然 IEEE 802.15.3a 通道已經被廣泛地採用，但是在這樣的通道下，超寬頻系統的效能評估大多是以模擬代替分析的方式來達成。在這類的超寬頻通道中所具有的獨特的群集 (cluster) 特性及高密度的多重路徑效應使得效能的分析變得有趣但也富有挑戰性。以數學的角度來看，在這樣的通道下的信號可視為一個聯合對數常態 (lognormal) 和帕松的隨機信號。其中信號振幅的衰減是以對數常態隨機變數來描述，而群集效應是以帕松隨機變數來描述。我們發展了一套計算位元錯誤率的方法，把所有 IEEE 802.15.3a 通道的參數都考慮進去，包括了群集/射線抵達率 (ray arrival rate)，群集/射線衰退因子 (decay factor)，每個群集所包含的射線數目，對數常態衰減和對數常態遮蔽效應。此外，耙式接收器 (RAKE receiver) 的耙齒數目也列入考慮。

二、在 IEEE 802.15.4a 通道下之耙式接受器之位元錯誤率分析

此一部分提供了在超寬頻通道下，應用耙式接收器接收反極 (antipodal) 和正交二元信號之位元錯誤率分析。我們提供了一個位元錯誤率的分析數學式以及計算的公式。我們考慮的通道模型是 IEEE 802.15.4a 通道。我們研究了所有參數所造成的影響，包括了群集抵達率，群集衰退常數 (cluster decay constant)，射線間抵達率 (inter-ray arrival rate)，射線衰退常數 (ray decay constant)，功率延遲模型 (power delay profile, PDP) 的參數，以及中上 (Nakagami) 衰減信號的分佈。對於 IEEE 802.15.4a 超寬頻通道而言，群集效應是以帕松隨機程序來描述，而射線間抵達時間是以超對數隨機變數來描述。我們提出了一個系統化的分析方法來評估超寬頻信號在這樣的一個跟連續的中上以及離散的帕松隨機變數有關的機率模型之下，它的數學統計特性。所以，我們所發展出來的分析模型可以有效率地計算出一個超寬頻信號在 IEEE 802.15.4a 通道下的位元錯誤率，來取代耗時的電腦程式模擬。

關鍵字：超寬頻 (Ultra-Wideband, UWB)，IEEE 802.15.3a 通道模型，IEEE 802.15.4a 通道模型，位元錯誤率 (bit error rate, BER)。

研究成果

第一部份的研究成果的一部份已發表至 IEEE Vehicular Technology Conference 2006 Spring [1]，完整的版本已投稿至 IEEE Transactions on Vehicular Technology [2]。第二部份的研究成果亦已被 IEEE Vehicular Technology Conference 2006 Fall [3] 所接受。詳見附件。

相關論文發表

[1] Wei-Cheng Liu and Li-Chun Wang, “Performance analysis of pulse based ultra-wideband systems in the highly frequency selective fading channel with cluster property,” to appear in *IEEE Vehicular Technology Conference 2006 Spring*.

[2] Wei-Cheng Liu and Li-Chun Wang, “Performance analysis of pulse based ultra-wideband systems in the highly frequency selective fading channel with random clusters and rays,” submitted to *IEEE Transactions on Vehicular Technology*.

[3] Wei-Cheng Liu and Li-Chun Wang, “BER analysis of the IEEE 802.15.4a channel model with RAKE receiver,” accepted by *IEEE Vehicular Technology Conference 2006 Fall*.

Performance Analysis of Pulse Based Ultra-Wideband Systems in the Highly Frequency Selective Fading Channel with Cluster Property

Wei-Cheng Liu and Li-Chun Wang
Department of Communication Engineering
National Chiao Tung University, Hsinchu, Taiwan
lichun@cc.nctu.edu.tw, Tel: +886-3-5712121 ext 54511

***Abstract*— This paper presents an analytical expression for the bit error rate (BER) of the antipodal and orthogonal binary signals in the ultra-wideband (UWB) channel, of which the unique characteristics include the cluster property and highly dense multipath effect. Specifically, we consider the IEEE 802.15.3a UWB channel and take into account of the impact of all the key parameters, consisting of the cluster arrival rate, cluster decay factor, the number of rays per cluster, and the distribution of a non-Rayleigh fading signal. For the IEEE 802.15.3a UWB channel, the effects of clustering are characterized by a Poisson discrete random variable, and the magnitude of the signal is modelled by lognormal random variable. In this paper, we develop an analytical model to compute the signal with such joint continuous lognormal and discrete Poisson random variable. Hence, the developed analytical model can be useful in evaluating the performance of an UWB signal in the IEEE 802.15.3a channel without time consuming simulations.**

***Index Terms*— Ultra-wideband (UWB), IEEE 802.15.3a channel model, bit error rate (BER).**

I. Introduction

WIRELESS systems continue pursuing even higher data rates and better quality. The ultra-wideband (UWB) is a promising technique to achieve this objective. Performance analysis of the UWB communication system in a realistic UWB channel is important but not an easy task.

In this work, we consider the IEEE 802.15.3a UWB channel model [1]. Two important properties distinguish the UWB channel from the conventional narrow band channel. First, the bandwidth of the UWB signals is much wider than the coherence bandwidth of the channel. Thus, in the frequency domain the extremely highly frequency selective fading occurs. Second, in the time domain the extremely large bandwidth leads to high resolution arrival time for the UWB signal. Thus, the reflected UWB waves by objects usually yield a number of clusters of rays, which may contain some non-Rayleigh multipath components.

A. Motivation

The challenges of analyzing UWB signals lie in three folds.

- First, unlike the narrow band channel model that usually has only one cluster with a fixed-number of arrival rays, the transmitted signal over the UWB channel may arrive in many clusters, of which the number of arrival rays is also random. Mathematically, the arrival process of the UWB signal is modelled by a doubly stochastic Poisson process. The collected signal energy at the RAKE receiver in a channel with unknown number of rays is difficult to be analyzed.
- The amplitude of the impulse response in the UWB channel is a joint two-dimension random variable, consisting of the lognormally faded amplitude with a mean related to two Erlang random variables. This is because the average of the channel impulse is also a random variable due to varying interarrival time of rays and clusters.
- Due to insufficient arrival rays in a very narrow time bin, the central limit theorem is no longer true. Thus, the multipath fading signal is not a traditional Rayleigh random variable. In the IEEE 802.15.3a UWB channel, the multipath fading signal is characterized by a lognormal random variable according to measurement results. Furthermore, shadowing is also considered in the IEEE 802.15.3a channel model. Thus, for a given number of rays and the mean of the signal amplitude, a UWB signal is a composite slowly varying lognormally shadowed/fast-varying lognormally faded random variable. The analysis of such a signal is rarely seen in current literature.

The IEEE 802.15.3a UWB channel model defines four sets of parameters for different environments. Based on this channel model, a UWB signal can be characterized by a joint continuous lognormal and discrete doubly stochastic Poisson random variable, of which key parameters include the cluster/ray arrival rates, the cluster/ray decay factors, the standard deviations of the lognormal fading.

To our knowledge, a complete analytical formula for the bit error rate (BER) performance with RAKE receiver in the IEEE 802.15.3a UWB channel considering all the three aforementioned challenges and key parameters is not seen in the literature.

B. Related Work

The published papers which are related to the performance analysis of the UWB system under different channels are listed as follows. In [2], the authors derived the theoretical BER

[1]This work is supported by the National Science Council, Taiwan, under the contract NSC94-2213-E-009-030.

of binary and M-ary UWB systems with Walsh codes under the AWGN channel with multiple access interference. In [3], the authors studied the performances of UWB systems in the AWGN channel in the presence of the interference from universal mobile telecommunications system (UMTS)/wideband code division multiple access (WCDMA) band is present. The BER performances of the UWB system were derived under the flat and dispersive Rayleigh fading channels with timing jitter in [4]. In [5], the authors analyzed the performance of a transmit-reference (TR) UWB system with a simple autocorrelation receiver under a slow fading channel of which attenuations are characterized by an appropriate moment generating function.

In [6], the authors derived a BER formula for the IEEE 802.15.3a UWB channel model but only as a function of finite window size rather than a function of the fingers number of the RAKE receiver. In [7], they further obtained statistics of the output SNR for the RAKE receiver in the IEEE 802.15.3a UWB channel, but without providing explicit BER formula and ignored the shadowing effect.

C. Objective and Outline of This Paper

The objective of this paper is to derive the analytical BER expression for the UWB system using the coherent RAKE receiver in a complete IEEE 802.15.3a UWB channel. The difference between [6] and [7] and our work are two folds. First, we consider the lognormal shadowing fading in the IEEE 802.15.3a channel model. Second, we derive the BER formula as a function of the fingers number of the RAKE receiver in the UWB channel. From the numerical results, we can see that BER in the IEEE 802.15.3a channel can be analyzed and approach the simulation results.

The rest of this paper is organized as follows. Section II describes the IEEE 802.15.3a channel model. In Section III, we derive the evaluation-form expression for BER of the binary signals subject to the impact of the considered UWB channel. Section IV shows our numerical results. Last, we give our conclusions in Section V.

II. Channel Model

We consider the UWB channel model in [1]. The impulse response of the channel model is

$$h_i(t) = X_i \sum_{l=0}^{N_c-1} \sum_{k=0}^{N_r-1} \alpha_{k,l}^i \delta(t - T_l^i - \tau_{k,l}^i), \tag{1}$$

where i refers to the i-th realization, $\{X_i\}$ represents the lognormal shadowing [i.e., $20\log(X_i) \propto \text{Normal}(0, \sigma_x^2)$], $\{\alpha_{k,l}^i\}$ are the multipath gain coefficients, $\{T_l^i\}$ is the delay of the l-th cluster, $\{\tau_{k,l}^i\}$ is the delay of the k-th multipath component relative to the l-th cluster arrival time (T_l^i), N_c is the number of clusters, and N_r is the number of rays for each cluster. By definition, we have $\tau_{0,l} = 0$.

The distribution of cluster arrival time and the ray arrival time are given by

$$p(T_l|T_{l-1}) = \Lambda \exp[-\Lambda(T_l - T_{l-1})] \tag{2}$$

and

$$p(\tau_{k,l}|\tau_{(k-1),l}) = \lambda \exp[-\lambda(\tau_{k,l} - \tau_{(k-1),l})] \tag{3}$$

where Λ and λ are the cluster and ray arrival rate, respectively. Note that $T_0 = 0$ in the line-of-sight (LOS) channel, while in the non-line-of-sight (NLOS) channel, T_0 is an exponential random variable. That is,

$$p(T_0) = \Lambda \exp(-\Lambda T_0). \tag{4}$$

The channel coefficients ($\alpha_{k,l}$) are defined as follows:

$$\alpha_{k,l} = p_{k,l}\xi_l\beta_{k,l}, \tag{5}$$

where $p_{k,l}$ is equiprobable ± 1 to account for signal inversion due to reflections, ξ_l reflects the fading associated with the l-th cluster, and $\beta_{k,l}$ corresponds to the fading associated with the k-th ray of the l-th cluster. The total energy contained in the terms $\{\alpha_{k,l}\}$ is normalized to unity for each realization. The distribution of $\xi_l\beta_{k,l}$ is

$$20\log(\xi_l\beta_{k,l}) \propto \text{Normal}(\mu_{k,l}, \sigma_1^2 + \sigma_2^2) \tag{6}$$

or

$$|\xi_l\beta_{k,l}| = 10^{(\mu_{k,l}+n_1+n_2)/20}, \tag{7}$$

where $n_1 \propto \text{Normal}(0, \sigma_1^2)$ and $n_2 \propto \text{Normal}(0, \sigma_2^2)$ are independent and correspond to the fading on each cluster and ray, respectively. Note that

$$\mu_{k,l} = \frac{10\ln(\Omega_0) - 10T_l/\Gamma - 10\tau_{k,l}/\gamma}{\ln(10)} - \frac{(\sigma_1^2 + \sigma_2^2)\ln(10)}{20} \tag{8}$$

and

$$\mathbb{E}[|\xi_l\beta_{k,l}|^2] = \Omega_0 e^{-T_l/\Gamma} e^{-\tau_{k,l}/\gamma}, \tag{9}$$

where Ω_0 is the mean energy of the first path of the first cluster and T_l is the excess delay of bin l. Γ is the cluster decay factor and γ is the ray decay factor.

In [1], through measurements, some initial parameters are given for four kinds of channel models, namely CM1, CM2, CM3, and CM4, which are based on LOS (0-4 m), NLOS (0-4 m), NLOS (4-10 m), and 25 nsec root-mean-square (RMS) delay spread channel measurements, respectively.

III. BER Analysis

A. Receiver Structure

We use a coherent RAKE receiver with L fingers. The received SNR γ_b is

$$\gamma_b = \frac{E_b}{N_0} \sum_{k=1}^{L} a_k^2 = \sum_{k=1}^{L} \gamma_k, \tag{10}$$

where E_b/N_0 is the bit SNR, a_k is the channel amplitude that appears at the k-th finger of the RAKE receiver. From [8] we know that the conditional error probability for binary signals for the coherent RAKE receiver is

$$P_2(\gamma_b) = Q\left(\sqrt{\gamma_b(1-\rho_r)}\right) \tag{11}$$

where $\rho_r = -1$ for antipodal signals and $\rho_r = 0$ for orthogonal signals. Next we will derive the characteristic function of the received energy $\mathcal{E} \triangleq \sum_{k=1}^{L} a_k^2$ in the UWB channel.

B. Characteristic Function of the Received Energy ($\mathcal{E}$)

In the following theorem, we give the formula of the characteristic function of $\mathcal{E}$. We exploit the result in [9] to further take the number of fingers of the RAKE receiver (L), the chip duration between two fingers (T_{c}), and shadowing into account. Importantly, instead of deriving the path gain of the UWB channel, we obtain directly the square of a path gain of a UWB channel, which can facilitate the BER calculation of the RAKE receiver in the UWB channel.

Corollary 1: Let $\mathcal{L}_{T,t}(\nu)$ be the characteristic function of the single path gain in the IEEE 802.15.3a UWB channel with the cluster arrival time at T and the ray arrival time at $t = T + \tau$. Also, denote $e^{-\lambda\psi_\nu(T)}$ and $e^{-\Lambda J(\nu)}$ the characteristic function of a shot-noise random variable related to the ray arrival process with parameter λ and that related to the cluster arrival process with parameter Λ, respectively. Then, it can be proved that the characteristic function of the received energy ($\mathcal{E}$) in the IEEE 802.15.3a UWB channel can be computed by

$$\Psi(\nu) = \mathcal{L}_{0,0}(\nu) e^{-\lambda\psi_\nu(0) - \Lambda J(\nu)}. \tag{12}$$

Proof: See [9]. ∎

Theorem 1: Consider a RAKE receiver with L fingers in the IEEE 802.15.3a UWB channel. The characteristic function $\mathcal{L}_{T,t}(\nu)$ can be computed by

$$\begin{aligned}\mathcal{L}_{T,t}(\nu) &= \int_0^\infty e^{j\nu x} \frac{10 \exp\left[-\frac{1}{8\sigma_{\mathcal{E}}^2}\left(20\log_{10} x - 2\mu_{T,t}\right)^2\right]}{\sqrt{2\pi}\sigma_{\mathcal{E}} x \ln 10} dx \\ &\approx \sum_{l=1}^{N^{(\mathrm{H})}} w_l^{(\mathrm{H})} \frac{1}{\sqrt{\pi}} \exp\left(j\nu 10^{\frac{\sqrt{2}\sigma_{\mathcal{E}} x_l^{(\mathrm{H})} + \mu_{T,t}}{10}}\right)\end{aligned} \tag{13}$$

where $\mu_{T,t} = \frac{10}{\ln 10}\left[\ln\Omega_0 - \frac{T}{\Gamma} - \frac{t-T}{\gamma} - \left(\frac{\ln 10}{10}\right)^2 \frac{\sigma_{\mathcal{E}}^2}{2}\right]$ and $\sigma_{\mathcal{E}} = \sqrt{\sigma_1^2 + \sigma_2^2 + \sigma_x^2}$. The parameters Ω_0, Γ, and γ are defined in (9). Note that $\sigma_{\mathcal{E}}$ consists of σ_1, σ_2, and σ_x, which represent the standard deviation of cluster fading, ray fading, and lognormal shadowing fading terms, respectively. $\{w_l^{(\mathrm{H})}\}$ and $\{x_l^{(\mathrm{H})}\}$ are the weights and abscissas of the Gauss-Hermite formula, respectively. $N^{(\mathrm{H})}$ is the number of points of the Gauss-Hermite integration.

Proof: See Appendix I. ∎

Theorem 2: For the RAKE receiver with L fingers, the function $\psi_\nu(T)$ in (12) can be computed by

$$\begin{aligned}&\psi_\nu(T) \\ &= \begin{cases} \int_T^{(L-1)T_{\mathrm{c}}} [1 - \mathcal{L}_{T,t}(\nu)] dt, & T \le (L-1)T_{\mathrm{c}}, \\ 0, & T > (L-1)T_{\mathrm{c}}, \end{cases} \\ &\approx \begin{cases} \frac{(L-1)T_{\mathrm{c}} - T}{2} \\ \sum_{p=1}^{N^{(\mathrm{L})}} w_p^{(\mathrm{L})} \left[1 - \mathcal{L}_{T,t}(\nu)\right]\Big| \\ \quad t = \frac{(L-1)T_{\mathrm{c}} - T}{2} x_p^{(\mathrm{L})} + \frac{(L-1)T_{\mathrm{c}} + T}{2}, & T \le (L-1)T_{\mathrm{c}}, \\ 0, & T > (L-1)T_{\mathrm{c}}, \end{cases}\end{aligned} \tag{14}$$

where T_{c} is the chip duration between two fingers, $\{w_p^{(\mathrm{L})}\}$ and $\{x_p^{(\mathrm{L})}\}$ are the weights and abscissas of the Gauss-Legendre formula, respectively. $N^{(\mathrm{L})}$ is the number of points of the Gauss-Legendre integration. Similarly, we can prove that $J(\nu)$ is equal to

$$\begin{aligned}J(\nu) &= \int_0^{(L-1)T_{\mathrm{c}}} [1 - \mathcal{L}_{T,T}(\nu) e^{-\lambda\psi_\nu(T)}] dT \\ &\approx \frac{(L-1)T_{\mathrm{c}}}{2} \sum_{i=1}^{N^{(\mathrm{L})}} w_i^{(\mathrm{L})} \left[1 - \mathcal{L}_{T,T}(\nu) e^{-\lambda\psi_\nu(T)}\right]\Big| \\ &\quad {\scriptstyle T = \frac{(L-1)T_{\mathrm{c}}}{2} x_i^{(\mathrm{L})} + \frac{(L-1)T_{\mathrm{c}}}{2}}.\end{aligned} \tag{15}$$

Proof: See Appendix II. ∎

With characteristic function of $\mathcal{E}$, i.e. $\Psi(\nu)$ in (12), the PDF of $\mathcal{E}$ can be computed by the Gauss-Hermite formula as follows:

$$\begin{aligned}f_{\mathcal{E}}(x) &= \frac{1}{2\pi}\int_{-\infty}^{\infty} \Psi(\nu) e^{-jx\nu} d\nu \\ &\approx \frac{1}{2\pi} \sum_{k=1}^{N^{(\mathrm{H})}} w_k^{(\mathrm{H})} \Psi(\nu) e^{-jx\nu} e^{\nu^2}\Big|_{\nu = x_k^{(\mathrm{H})}}.\end{aligned} \tag{16}$$

Combining (13), (14), (15), and (16), the BER of the RAKE receiver in the IEEE 802.15.3a UWB channel can be computed as

$$\begin{aligned}P_2 &= \mathbb{E}_{\mathcal{E}}\left[Q\left(\sqrt{(1-\rho_r)\frac{E_{\mathrm{b}}}{N_0}\mathcal{E}}\right)\right] \\ &= \int_0^\infty Q\left(\sqrt{(1-\rho_r)\frac{E_{\mathrm{b}}}{N_0}x}\right) f_{\mathcal{E}}(x) dx \\ &= \frac{1}{2\pi^{3/2}} \sum_{k=1}^{N^{(\mathrm{H})}} \sum_{l=1}^{N^{(\mathrm{H})}} w_k^{(\mathrm{H})} w_l^{(\mathrm{H})} \exp\left(j\nu 10^{\frac{\sqrt{2}\sigma_{\mathcal{E}} x_l^{(\mathrm{H})} + \mu_{0,0}}{10}}\right) \\ &\quad \exp\left(-\frac{1}{2}\lambda(L-1)T_{\mathrm{c}} \sum_{p=1}^{N^{(\mathrm{L})}} w_p^{(\mathrm{L})} \left[1 - \mathcal{L}_{0,t}(\nu)\right]\right| \\ &\quad {\scriptstyle t = \frac{1}{2}(L-1)T_{\mathrm{c}}(x_p^{(\mathrm{L})}+1)}\Big) \exp\left(-\frac{1}{2}\Lambda(L-1)T_{\mathrm{c}} \sum_{i=1}^{N^{(\mathrm{L})}} w_i^{(\mathrm{L})}\right. \\ &\quad \left.\left[1 - \mathcal{L}_{T,T}(\nu) e^{-\lambda\psi_\nu(T)}\right]\Big|_{T = \frac{1}{2}(L-1)T_{\mathrm{c}}(x_i^{(\mathrm{L})}+1)}\right) \\ &\quad \int_0^\infty Q\left(\sqrt{(1-\rho_r)\frac{E_{\mathrm{b}}}{N_0}x}\right) \\ &\quad \exp(-jx\nu) dx \exp(\nu^2)\big|_{\nu = x_k^{(\mathrm{H})}}.\end{aligned} \tag{17}$$

Compared to [9], we further consider the impact of parameters L, T_{c}, σ_x^2, and the characteristic function of the square of the path gain into our formula. Also, an explicit computation formula is provided.

IV. Numerical Results

A. Simulation Method

In order to check the correctness of the BER formula in the last section, we perform simulation by using MATLAB. We consider the orthogonal binary signal, i.e. the PPM signal. When the information bit is 0, the transmitted signal is

$$s_0(t) = \begin{cases} 1, & 0 \le t < T_{\mathrm{c}}, \\ 0, & \text{otherwise}. \end{cases} \tag{18}$$

Here we set $T_c = 1$ nsec. When the information bit is 1, the signal waveform is $s_1(t) = s_0(t - \delta T_c)$, where δ is a positive integer. From the `uwb_sv_model_ct` function in [1], we can get the output vectors $\mathbf{h}$ and $\mathbf{t}$. The vector $\mathbf{t}$ stores the arrival time of every channel impulse response with increasing chronological order. The vector $\mathbf{h}$ stores the corresponding amplitude.

We define a template vector $\mathbf{p}_0$ with size $1 \times (L+\delta)$, where the m-th element of $\mathbf{p}_0$ (denote by $\mathbf{p}_0[m]$) is equal to

$$\mathbf{p}_0[m] = \begin{cases} \sum_{n:\mathbf{t}[n]=0} \mathbf{h}[n], & m = 1, \\ \sum_{n:(m-2)T_c<\mathbf{t}[n]\le(m-1)T_c} \mathbf{h}[n], & 2 \le m \le L, \\ 0, & L < m \le L+\delta. \end{cases} \tag{19}$$

The physical meaning of the vector $\mathbf{p}_0$ is the received signal excluding the noise sampled at a rate of $1/T_c$ given the information bit being 0. If the information bit is 1, then the template vector can be expressed as $\mathbf{p}_1[m] = [\mathbf{0}_{1\times\delta}, \mathbf{p}_0[1], \cdots, \mathbf{p}_0[L]]$.

After adding noise $\mathbf{n}$, the sampled received signal for information bit 0 becomes $\mathbf{r} = \mathbf{p}_0 + [\mathbf{n}, \mathbf{0}_{1\times\delta}]$ and that for information bit 1 is $\mathbf{r} = \mathbf{p}_1 + [\mathbf{0}_{1\times\delta}, \mathbf{n}]$. Note that the noise vector $\mathbf{n}$ contains L independent identically distributed normal random variables, each of which has zero mean and variance of $N_0/2$.

The coherent RAKE receiver is applied to detect the signal in the IEEE 802.15.3a UWB channel. Let the decision variable $U_0 = \mathbf{r}\cdot\mathbf{p}_0$ and $U_1 = \mathbf{r}\cdot\mathbf{p}_1$, where the operator "$\cdot$" is the inner product of two vectors. If $U_0 \ge U_1$, then the information bit is 0, otherwise the information bit is 1.

B. Results

Figure 1 compares the BER performance based on (7) in [6] and (17) in our paper. For the BER curve based on [6], we reproduce the curve in [6, Fig. 1], where the received waveform is observed only over a finite window $[0, T_{\max}]$ and $T_{\max} = 33$ nsec. The symbol $\eta = \mathcal{E}_w/(8\sigma_n^2)$, where $\mathcal{E}_w$ is the signal energy of and σ_n^2 is the noise power spectral density. In the figure, we observe that the BER based on (17) is slightly higher than that based on (7) of [6]. This is because we take the lognormal shadowing into account.

Figure 2 shows the BER v.s. E_b/N_0 for CM1, CM2, CM3, and CM4 by simulation and analysis. For the analytical curves, We consider the orthogonal binary signal, i.e., $\rho_r = 0$. The parameter δ of the PPM is set to be one. The number of the fingers of the RAKE receiver is 10. The space of the fingers of the RAKE receiver, T_c, is set to 1 nsec. For each given E_b/N_0, we simulate 100,000 bits to obtain the BER. As seen from the figure, the analytical results match the simulation results quite well. However, for CM3 and CM4, there are some differences between the simulation and the analytical curves, which may result from the following reasons:

1) The usage of Gauss-Hermite and Gauss-Legendre formulae may cause some error in integrations.
2) We use the MATLAB programs provided in [1] to generate the IEEE 802.15.3a channel. Theoretically the Poisson process has infinite arrivals, but the computer simulation can only generate finite arrivals. The MATLAB program in [1] only produces the clusters with the arrival time up to 10Γ. Meanwhile, each cluster only contains the rays with the arrival time up to 10γ. Thus, the RAKE receiver in the simulation may collect less energy than that in the ideal case. Thus the simulation BER values are slightly higher than the theoretical BER values.

V. Conclusions

In this work, we have derived the BER analytical formula for receiving the antipodal and orthogonal binary signals by using a coherent RAKE receiver over the IEEE 802.15.3a UWB channel model. Our numerical results show that the simulation and the analytical values of the BER are very close. Using our analytical BER formula can save computer simulation time. Furthermore, the suggested analytical method can be applied to other multipath channel models.

The possible future works that can be extended from this work include the following. First, we plan to analyze the same problem under the IEEE 802.15.4a UWB channel model [10]. Second, we are going to find the ergodic capacity of such a UWB channel models.

Appendix I
Proof of Theorem 1

Let $f_{G|T,t}(x)$ be the PDF of the path gain $G \triangleq \alpha_{k,l}$ arriving at time t that is part of a cluster that started at time T. According to [9], $f_{G|T,t}(x)$ can be written as

$$f_{G|T,t}(x) = \frac{1}{2}[f_{|G||T,t}(x) + f_{|G||T,t}(-x)], \tag{20}$$

because the path gain has probability of $1/2$ being positive and probability of $1/2$ being negative [Recall the definition of path gain in (5) and the following context.] Note that $f_{|G||T,t}(x)$ is lognormally distributed, i.e.,

$$f_{|G||T,t}(x) = \begin{cases} \frac{20\exp\left[-\frac{1}{2\sigma^2}(20\log_{10}x - \mu_{T,t})^2\right]}{\sqrt{2\pi}\sigma x \ln 10}, & x > 0, \\ 0, & \text{otherwise.} \end{cases} \tag{21}$$

where $\mu_{T,t}$ is given in (1) and $\sigma = \sqrt{\sigma_1^2 + \sigma_2^2}$ are the mean and variance of the random variable $20\log_{10}|G|$, respectively. Note that (1) is the continuous-time representation of (8), because we have changed the discrete indices k and l to continuous arrival time t and T, respectively.

The complete form of the square path gain should be X^2G^2, where X is the lognormal shadowing introduced in Section II. Since $20\log_{10}X \propto \text{Normal}(0, \sigma_x^2)$, we have

$$20\log_{10}X^2 = 2(20\log_{10}X) \propto \text{Normal}(0, (2\sigma_x)^2) \tag{22}$$

and then

$$\begin{aligned} & 20\log_{10}X^2G^2 \\ = \;& 2(20\log_{10}X|G|) \\ = \;& 2(20\log_{10}X) + 2(20\log_{10}|G|) \\ \propto \;& \text{Normal}(0, (2\sigma_x)^2) + \text{Normal}(2\mu_{T,t}, (2\sigma)^2) \\ \propto \;& \text{Normal}(2\mu_{T,t}, 4(\sigma_1^2 + \sigma_2^2 + \sigma_x^2)). \end{aligned} \tag{23}$$

Define $\sigma_{\mathcal{E}} = \sqrt{\sigma_1^2 + \sigma_2^2 + \sigma_x^2}$. Then the PDF of the square of the path gain arriving at time t that is part of a cluster that started at time T can be written as

$$f_{T,t}(x) = \begin{cases} \frac{10 \exp\ -\frac{1}{8\sigma_{\mathcal{E}}^2}(20\log_{10} x - 2\mu_{T,t})^2}{\sqrt{2\pi}\sigma_{\mathcal{E}} x \ln 10}, & x > 0, \\ 0, & \text{otherwise.} \end{cases} \tag{24}$$

Denote $\mathcal{L}_{T,t}(\nu)$ as the characteristic function of $f_{T,t}(x)$, i.e.,

$$\mathcal{L}_{T,t}(\nu) = \mathbb{E}_{T,t}[e^{j\nu X^2 G^2}] = \int_{-\infty}^{\infty} e^{j\nu x} f_{T,t}(x) dx. \tag{25}$$

Let $y = \frac{1}{2\sqrt{2}\sigma_{\mathcal{E}}}(20\log_{10} x - 2\mu_{T,t})$ and apply it to (13). Then we can have

$$\begin{aligned} & \mathcal{L}_{T,t}(\nu) \\ = & \int_{-\infty}^{\infty} \exp\left(j\nu 10^{\frac{2\sqrt{2}\sigma_{\mathcal{E}} y + 2\mu_{T,t}}{20}}\right) \frac{10e^{-y^2}}{\sqrt{2\pi}\sigma_{\mathcal{E}} x \ln 10} \frac{x\sigma_{\mathcal{E}} \ln 10}{5\sqrt{2}} dy \\ = & \int_{-\infty}^{\infty} \frac{1}{\sqrt{\pi}} \exp\left(j\nu 10^{\frac{\sqrt{2}\sigma_{\mathcal{E}} y + \mu_{T,t}}{10}}\right) e^{-y^2} dy \\ \approx & \sum_{l=1}^{N^{(\mathrm{H})}} w_l^{(\mathrm{H})} \frac{1}{\sqrt{\pi}} \exp\left(j\nu 10^{\frac{\sqrt{2}\sigma_{\mathcal{E}} x_l^{(\mathrm{H})} + \mu_{T,t}}{10}}\right). \end{aligned} \tag{26}$$

Appendix II
Proof of Theorem 2

In [9] the authors have obtained the characteristic function of the sum of path gains in the time window $[a, b]$ (denoted by Φ), but the lognormal shadowing is not taken into account. Similarly, we apply their results to determine the characteristic function of $\mathcal{E}$. Assume that the RAKE receiver with L fingers is used to collect the channel energy in the time window $[0, (L-1)T_{\mathrm{c}}]$, where T_{c} is the chip duration between two fingers.

In [9], the authors defined the following functions:

$$\psi_\nu(T) = \begin{cases} \int_{\max(a,T)}^{b} [1 - \mathcal{L}_{T,t}(\nu)] dt, & T \le b, \\ 0, & T > b, \end{cases} \tag{27}$$

and

$$J(\nu) = \int_0^a [1 - e^{-\lambda\psi_\nu(T)}] dT + \int_0^b [1 - \mathcal{L}_{T,T}(\nu) e^{-\lambda\psi_\nu(T)}] dT. \tag{28}$$

We set $a = 0$, $b = (L-1)T_{\mathrm{c}}$, and use the Gauss-Legendre formula [11]. Then we can transform the above equations to (14) and (15), respectively.

References

[1] J. Foerster, et. al., "Channel modeling sub-committee report final," *IEEE P802.15 Wireless Personal Area Networks, P802.15-02/490r1-SG3a*, Feb. 2003.

[2] K. Eshima, Y. Hase, S. Oomori, F. Takahashi, and R. Kohno, "M-ary UWB system using Walsh codes," *IEEE Conference on Ultra Wideband Systems and Technologies*, pp. 37–40, May 21–23, 2002.

[3] M. Hämäläinen, R. Tesi, and J. Iinatti, "On the UWB system performance studies in AWGN channel with interference in UMTS band," *IEEE Conference on Ultra Wideband Systems and Technologies*, pp. 321–325, May 21–23, 2002.

[4] İ. Güvenç and H. Arslan, "Performance evaluation of UWB systems in the presence of timing jitter," *IEEE Conference on Ultra Wideband Systems and Technologies*, pp. 136–141, Nov. 16–19, 2003.

[5] T. Q. S. Quek and M. Z. Win, "Ultrawide bandwidth transmitted-reference signaling," *IEEE International Conference on Communications*, vol. 6, pp. 3409–3413, June 20–24, 2004.

[6] J. A. Gubner and K. Hao, "A computable formula for the average bit-error probability as a function of window size for the IEEE 802.15.3a UWB channel model," *IEEE Trans. Microwave Theory Tech.*, submitted for publication. [Online]. Available: http://homepages.cae.wisc.edu/~gubner/GubnerHao_MTT_UWB.pdf

[7] K. Hao and J. A. Gubner, "Performance measures and statistical quantities of rake receivers using maximal-ratio combining on the IEEE 802.15.3a UWB channel model," *IEEE Trans. Wireless Commun.*, submitted for publication. [Online]. Available: http://homepages.cae.wisc.edu/~gubner/HaoGubnerTWaf2col.pdf

[8] J. G. Proakis, *Digital Communications*, 4th ed. Boston: McGraw-Hill, 2001.

[9] K. Hao and J. A. Gubner, "The distribution of sums of path gains in the IEEE 802.15.3a UWB channel model," *IEEE Trans. Wireless Commun.*, submitted for publication. [Online]. Available: http://homepages.cae.wisc.edu/~gubner/HaoGubnerTWireless2col.pdf

[10] A. F. Molisch et al., "IEEE 802.15.4a channel model - final report," IEEE 802.15 WPAN Low Rate Alternative PHY Task Group 4a (TG4a), Tech. Rep., Nov. 2004.

[11] [Online]. Available: http://www.efunda.com/math/num_integration/num_int_gauss.cfm

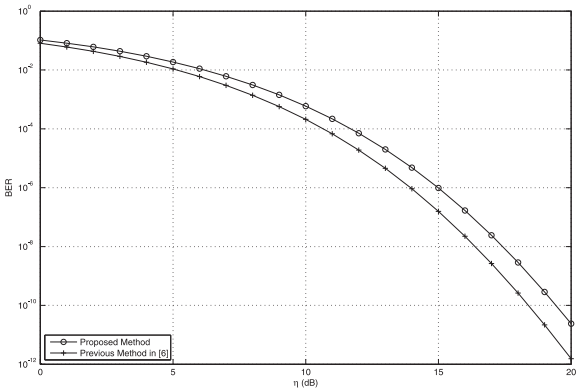

Fig. 1. BER comparison of the proposed analytical formulae with that in [6], where $T_{\max} = 33$ nsec.

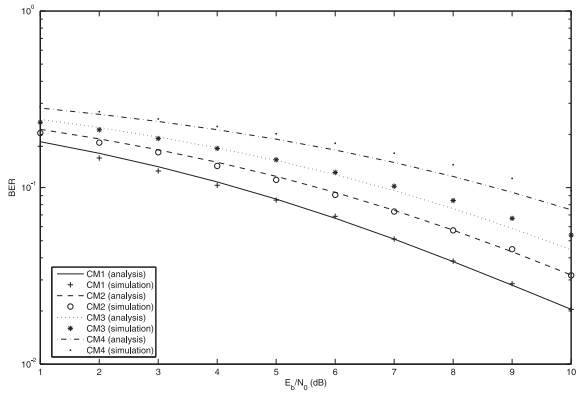

Fig. 2. The BER v.s. E_{b}/N_0 for the RAKE receiver with 10 fingers in the IEEE 802.15.3a UWB channels CM1, CM2, CM3, and CM4.

Performance Analysis of Pulse Based Ultra-Wideband Systems in the Highly Frequency Selective Fading Channel with Random Clusters and Rays

Wei-Cheng Liu and Li-Chun Wang
Department of Communication Engineering
National Chiao Tung University, Hsinchu, Taiwan
lichun@cc.nctu.edu.tw, Tel: +886-3-5712121 ext 54511

***Abstract*— In this paper, an analytical expression for the bit error rate (BER) of binary signals in the IEEE 802.15.3a ultra-wideband (UWB) channel is presented. Although the IEEE 802.15.3a channel model is widely adopted, the performance of UWB system in such a channel are mainly evaluated by simulations instead of analysis. The unique characteristics of cluster property and highly dense multipath effect make performance analysis in this kind of UWB channel interesting but challenging. Mathematically, the signal in such a UWB channel can be characterized by a joint lognormal and Poisson random signal, where the lognormal random variable models the fading amplitude and the Poisson random variable model the clustering effect. We develop a BER computation method to take into account of all the key parameters in the IEEE 802.15.3a UWB channel, consisting of the cluster/ray arrival rate, cluster/ray decay factor, the number of rays per cluster, lognormal fading and lognormal shadowing. Furthermore, the effect of finger numbers of the RAKE receiver is also considered.**

***Index Terms*— Ultra-wideband (UWB), IEEE 802.15.3a channel model, bit error rate (BER).**

I. Introduction

ULTRA-WIDEBAND (UWB) is a promising technique for wireless communications due to its high speed transmission. However, the UWB channel characteristics are very different from the conventional narrowband channel. Currently, most UWB systems are evaluated by simulations in the complicated channel model or by analysis in a simplified channel model.

Thus a fundamental question arises: Can a UWB system be possibly analyzed in a more realistic UWB channel model? The IEEE 802.15.3a UWB channel model [1] is widely adopted for the product development in the industry, while the analysis under such a channel is rarely seen in the literature. This UWB channel has two important properties different from the conventional narrowband channel. First, the extremely highly frequency selective fading occurs in the frequency domain because the UWB signal occurs is much wider than the channel coherence bandwidth. Second, the UWB signals reflected by objects usually yield a number of clusters of rays and contain some non-Rayleigh multipath components because the extremely large bandwidth in the time domain leads to the high-resolution arrival time.

[1]This work was supported by the National Science Council, Taiwan, under the contract NSC94-2213-E-009-030.

A. Problem Statement

The challenges of analyzing such UWB signals can be explained in the following three folds.

- Unlike the narrowband channel model with only one cluster of fixed-number arrival rays, the transmitted signal over the UWB channel may arrive in many clusters with a random number of arrival rays. Mathematically, the arrival process of the UWB signal can be modeled by a doubly stochastic Poisson process. For a channel with an unknown number of rays, it is difficult to compute how much signal energy is collected at the RAKE receiver.
- The UWB channel presents the characteristics of a log-normally faded amplitude with a mean related to two Erlang random variables for varying arrival time of rays and clusters. Signal analysis for such a joint two-dimension random variable is not straightforward.
- Because insufficient arrival rays in a very narrow time bin cannot justify the assumption of the central limit theorem, the multipath fading signal is not a traditional Rayleigh random variable in the UWB channel. According to measurement results, the IEEE 802.15.3a UWB channel adopts a lognormal multipath fading signal. In addition, shadowing is also considered in the IEEE 802.15.3a channel model. Thus, a UWB signal is a composite slowly varying lognormally shadowed/fast-varying lognormally faded random variable conditioned on the given number of rays and the given signal amplitude's mean. Again, the analysis of such a signal is rarely seen in the current literature.

In short, a UWB signal in the IEEE 802.15.3a channel model can be characterized by a joint lognormal and doubly stochastic Poisson random variable with key parameters including cluster/ray arrival rates, cluster/ray decay factors, and the standard deviations of the lognormal fading and shadowing. To our knowledge, a complete analytical bit error

rate (BER) computation formula for the RAKE receiver in the IEEE 802.15.3a UWB channel is not seen in the literature.

B. Related Work

In the following we briefly summarize some published papers in the literature related to the performance analysis of the UWB system under different channels. In [2], the authors derived the theoretical BER of binary and M-ary UWB systems with Walsh codes under the AWGN channel and multiple access interference.

On the one hand, in [3]–[5], the UWB system was investigated in certain simplified UWB channel models. In [3], the authors studied the performances of UWB systems in the AWGN channel in the presence of the interference from the wideband code division multiple access (WCDMA) of the universal mobile telecommunications system (UMTS). The BER performances of the UWB system under the flat and dispersive Rayleigh fading channels with timing jitter were derived in [4]. In [5], based on an approach of defining channel amplitude by a moment generating function, the authors analyze the performance of a transmit-reference (TR) UWB system with a simple autocorrelation receiver under a slow fading channel.

On the other hand, the following papers considered more sophisticated UWB channels [6]–[9]. With respect to the IEEE 802.15.3a channel model, [6] derived a BER formula as a function of the window size. In [7], they further investigated the statistics of the output SNR at the RAKE receiver. Reference [8] analyzed how multiple transmit and receive antennas affect the SNR of the UWB signal under a channel characterized by 1) a Gamma distributed path power; 2) a modified Poisson process for modeling the number of the simultaneously arriving paths; 3) an exponentially decayed resolvable path power in the time domain. In [9], the analytical error performance of a multi-antenna with a zero-forcing (ZF) RAKE receiver system over the frequency-selective UWB lognormal fading channels was analyzed.

However, to our knowledge, an explicit BER analytical computation method incorporating the impact of the finger number of the RAKE receiver as well as shadowing effect in the IEEE 802.15.3a UWB channel has not been seen in the literature.

C. Objective and Outline of This Paper

The objective of this paper is to develop an analytical method to compute the BER for the UWB system with a coherent RAKE receiver in a complete IEEE 802.15.3a channel. The difference between [6] and [7] and our work are two folds. First, we consider the lognormal shadowing fading as specified in the IEEE 802.15.3a channel model. Second, we derive an explicit BER formula as a function of the fingers number of the RAKE receiver. The rest of this paper is organized as follows. Section II introduces the IEEE 802.15.3a channel model. In Section III, we derive the expression for evaluating the BER of the binary signals subject to the impact of the considered UWB channel. Section IV shows our numerical results. Last, we give our conclusions in Section V.

II. Channel Model

In this section, we discuss the key attributes of the IEEE 802.15.3a UWB channel [1]. The impulse response of the considered channel model is

$$h_i(t) = X_i \sum_{l=0}^{N_c-1} \sum_{k=0}^{N_r-1} \alpha_{k,l}^i \delta(t - T_l^i - \tau_{k,l}^i) \ , \tag{1}$$

where i refers to the i-th realization, X_i represents the log-normal shadowing (i.e., $20\log(X_i) \propto \text{Normal}(0, \sigma_x^2)$), $\{\alpha_{k,l}^i\}$ are the multipath gain coefficients, T_l^i is the delay of the l-th cluster, $\tau_{k,l}^i$ is the delay of the k-th multipath component relative to the l-th cluster arrival time (T_l^i), N_c is the number of clusters, and N_r is the number of rays for each cluster. By definition, we have $\tau_{0,l} = 0$.

The distribution of the cluster arrival time and ray arrival time are given by

$$p(T_l|T_{l-1}) = \begin{cases} \Lambda \exp[-\Lambda(T_l - T_{l-1})], & T_l > T_{l-1}, \\ 0, & \text{otherwise}, \end{cases} \tag{2}$$

for $l > 0$, and

$$\begin{aligned} & p(\tau_{k,l}|\tau_{(k-1),l}) \\ = & \begin{cases} \lambda \exp[-\lambda(\tau_{k,l} - \tau_{(k-1),l})], & \tau_{k,l} > \tau_{(k-1),l}, \\ 0, & \text{otherwise}, \end{cases} \end{aligned} \tag{3}$$

for $k > 0$, where Λ and λ are the cluster and ray arrival rates, respectively. Note that $T_0 = 0$ in the line-of-sight (LOS) channel. T_0 is an exponential random variable in the non-line-of-sight (NLOS) channel, i.e.,

$$p(T_0) = \begin{cases} \Lambda \exp(-\Lambda T_0), & T_0 > 0, \\ 0, & \text{otherwise}. \end{cases} \tag{4}$$

The channel coefficients ($\alpha_{k,l}$) are defined as follows:

$$\alpha_{k,l} = p_{k,l} \xi_l \beta_{k,l} \ , \tag{5}$$

where $p_{k,l}$ is equiprobable ± 1 to account for signal inversion due to reflections, ξ_l reflects the fading associated with the l-th cluster, and $\beta_{k,l}$ corresponds to the fading associated with the k-th ray of the l-th cluster. The total energy contained in the terms $\{\alpha_{k,l}\}$ is normalized to unity for each realization. The distribution of $\xi_l \beta_{k,l}$ is

$$20\log(\xi_l \beta_{k,l}) \propto \text{Normal}(\mu_{k,l}, \sigma_1^2 + \sigma_2^2) \tag{6}$$

or

$$|\xi_l \beta_{k,l}| = 10^{(\mu_{k,l} + n_1 + n_2)/20} \ , \tag{7}$$

where the two independent normal random variables n_1 and n_2 with variance of σ_1^2 and σ_2^2 represent the fading on each cluster and ray in the dB domain, respectively. Note that

$$\mu_{k,l} = \frac{10\ln(\Omega_0) - 10T_l/\Gamma - 10\tau_{k,l}/\gamma}{\ln(10)} - \frac{(\sigma_1^2 + \sigma_2^2)\ln(10)}{20} \tag{8}$$

and

$$\mathbb{E}[|\xi_l \beta_{k,l}|^2] = \Omega_0 e^{-T_l/\Gamma} e^{-\tau_{k,l}/\gamma}, \tag{9}$$

where Ω_0 is the mean energy in the first path of the first cluster and T_l is the excess delay of bin l, Γ is the cluster decay factor, and γ is the ray decay factor.

Through measurements in [1], some parameters in the IEEE 802.15.3a channel are specified for four different environments, i.e., CM1, CM2, CM3, and CM4 for LOS (0-4 m), NLOS (0-4 m), NLOS (4-10 m), and extreme NLOS multipath channel with 25 nsec rms delay spread, respectively.

III. BER Analysis

A. Receiver Structure

For a coherent RAKE receiver with L fingers, the received SNR γ_b is

$$\gamma_b = \frac{E_\mathrm{b}}{N_0}\sum_{k=1}^{L} a_k^2 = \sum_{k=1}^{L}\gamma_k \ , \tag{10}$$

where E_b/N_0 is the bit SNR, a_k is the channel amplitude at the k-th finger of the RAKE receiver. From [10] we know that the conditional error probability for binary signals for the coherent RAKE receiver is

$$P_2(\gamma_b) = Q\left(\sqrt{\gamma_b(1-\rho_r)}\right) \ , \tag{11}$$

where $\rho_r = -1$ for antipodal signals and $\rho_r = 0$ for orthogonal signals. Denote $\mathcal{E} \triangleq \sum_{k=1}^{L} a_k^2$ the received energy in the UWB channel.

B. Characteristic Function of the Received Energy ($\mathcal{E}$)

Here we derive the characteristic function of $\mathcal{E}$. We extend the results in [11] to further take into account of the finger numbers of the RAKE receiver (L), the chip duration (T_c), and shadowing. Instead of estimating the path gain, we directly calculate the square of a path gain in the UWB channel to facilitate the BER evaluation of the RAKE receiver in the UWB channel.

Corollary 1: The received energy $\mathcal{E}$ has the following properties: $\mathcal{E}$ can be written as the sum of three statistically independent terms

$$\mathcal{E} = X^2\alpha_{0,0}^2 + \Phi_{r0} + \Phi_{\otimes} \ , \tag{12}$$

where X and $\alpha_{0,0}$ are defined in (1), Φ_{r0} is the energy of the first cluster excluding the first ray, $\Phi_{\otimes}$ is the total energy of the remaining clusters. Then, the characteristic function of the received energy ($\mathcal{E}$) in the IEEE 802.15.3a UWB channel is

$$\Psi(\nu) = \mathcal{L}_{0,0}(\nu)R(\nu)S(\nu), \tag{13}$$

where $\mathcal{L}_{T,t}(\nu)$ is the characteristic function of the single path squared gain in the IEEE 802.15.3a UWB channel with the cluster arriving at time T and the ray arriving at $T+\tau$, $R(\nu)$ and $S(\nu)$ are the characteristic functions of Φ_{r0} and $\Phi_{\otimes}$, respectively.

Proof: See [11]. ∎

Compared to [11], we further consider the impact of parameters L, T_c, σ_x^2, and the characteristic function of the square of the path gain into $\mathcal{L}_{T,t}(\nu)$, $R(\nu)$, and $S(\nu)$. Also, explicit computation formulas are provided.

Theorem 1: Consider a RAKE receiver with L fingers in the IEEE 802.15.3a UWB channel. The characteristic function $\mathcal{L}_{T,t}(\nu)$ can be computed by

$$\begin{aligned}\mathcal{L}_{T,t}(\nu) &= \int_0^\infty e^{j\nu x}\frac{10\exp\left[-\frac{1}{8\sigma_\mathcal{E}^2}\left(20\log_{10}x - 2\mu_{T,t}\right)^2\right]}{\sqrt{2\pi}\sigma_\mathcal{E} x\ln 10}dx \\ &\approx \sum_{l=1}^{N^{(\mathrm{H})}} w_l^{(\mathrm{H})}\frac{1}{\sqrt{\pi}}\exp\left(j\nu 10^{\frac{\sqrt{2}\sigma_\mathcal{E}x_l^{(\mathrm{H})}+\mu_{T,t}}{10}}\right)\end{aligned} \tag{14}$$

where

$$\mu_{T,t} = \frac{10}{\ln 10}\left[\ln\Omega_0 - \frac{T}{\Gamma} - \frac{t-T}{\gamma} - \left(\frac{\ln 10}{10}\right)^2\frac{\sigma_\mathcal{E}^2}{2}\right] \tag{15}$$

and

$$\sigma_\mathcal{E} = \sqrt{\sigma_1^2+\sigma_2^2+\sigma_x^2} \quad . \tag{16}$$

The parameters Ω_0, Γ, and γ are defined in (9). Note that $\sigma_\mathcal{E}$ consists of σ_1, σ_2, and σ_x, which represent the standard deviation of cluster fading, ray fading, and lognormal shadowing fading terms, respectively. $\{w_l^{(\mathrm{H})}\}$ and $\{x_l^{(\mathrm{H})}\}$ are the weights and abscissas of the Gauss-Hermite formula [12], respectively. $N^{(\mathrm{H})}$ is the number of points of the Gauss-Hermite integration.

Proof: See Appendix I. ∎

Theorem 2: For the RAKE receiver with L fingers, the function $R(\nu)$ in (13) can be written in the form of

$$R(\nu) = e^{-\lambda\psi_\nu(0)} \ , \tag{17}$$

where the function $\psi_\nu(T)$ can be computed by

$$\begin{aligned}&\psi_\nu(T) \\ &= \begin{cases}\int_T^{(L-1)T_\mathrm{c}}[1-\mathcal{L}_{T,t}(\nu)]dt, & T \le (L-1)T_\mathrm{c}, \\ 0, & T > (L-1)T_\mathrm{c},\end{cases} \\ &\approx \begin{cases}\frac{(L-1)T_\mathrm{c}-T}{2}\sum_{p=1}^{N^{(\mathrm{L})}} w_p^{(\mathrm{L})}\left[1-\mathcal{L}_{T,t}(\nu)\right] & \\ \quad\Big|_{t=\frac{(L-1)T_\mathrm{c}-T}{2}x_p^{(\mathrm{L})}+\frac{(L-1)T_\mathrm{c}+T}{2}}, & T \le (L-1)T_\mathrm{c}, \\ 0, & T > (L-1)T_\mathrm{c},\end{cases}\end{aligned} \tag{18}$$

where T_c is the chip duration between two fingers, $\{w_p^{(\mathrm{L})}\}$ and $\{x_p^{(\mathrm{L})}\}$ are the weights and abscissas of the Gauss-Legendre formula [12], respectively. $N^{(\mathrm{L})}$ is the number of points of the Gauss-Legendre integration. Similarly, we can prove that $S(\nu)$ can be written in the form of

$$S(\nu) = e^{-\Lambda J(\nu)} \ , \tag{19}$$

where the function $J(\nu)$ can be computed by

$$\begin{aligned}J(\nu) &= \int_0^{(L-1)T_\mathrm{c}}[1-\mathcal{L}_{T,T}(\nu)e^{-\lambda\psi_\nu(T)}]dT \\ &\approx \frac{(L-1)T_\mathrm{c}}{2}\sum_{i=1}^{N^{(\mathrm{L})}} w_i^{(\mathrm{L})}\left[1-\mathcal{L}_{T,T}(\nu)e^{-\lambda\psi_\nu(T)}\right] \\ &\quad\Big|_{T=\frac{(L-1)T_\mathrm{c}}{2}x_i^{(\mathrm{L})}+\frac{(L-1)T_\mathrm{c}}{2}} .\end{aligned} \tag{20}$$

Proof: See Appendix II. ∎

With the characteristic function $\Psi(\nu)$ of $\mathcal{E}$, the PDF of $\mathcal{E}$ can be computed by the Gauss-Hermite formula as follows:

$$\begin{aligned} f_{\mathcal{E}}(x) &= \frac{1}{2\pi}\int_{-\infty}^{\infty}\Psi(\nu)e^{-jx\nu}d\nu \\ &\approx \frac{1}{2\pi}\sum_{k=1}^{N^{(\mathrm{H})}} w_k^{(\mathrm{H})}\Psi(\nu)e^{-jx\nu}e^{\nu^2}\Big|_{\nu=x_k^{(\mathrm{H})}}. \end{aligned} \quad (21)$$

Combining (14), (18), (20), and (21), the BER of the RAKE receiver in the IEEE 802.15.3a UWB channel can be computed as

$$\begin{aligned} & P_2 \\ =\ & \mathbb{E}_{\mathcal{E}}\left[Q\left(\sqrt{(1-\rho_r)\frac{E_\mathrm{b}}{N_0}\mathcal{E}}\right)\right] \\ =\ & \int_0^\infty Q\left(\sqrt{(1-\rho_r)\frac{E_\mathrm{b}}{N_0}x}\right)f_{\mathcal{E}}(x)dx \\ =\ & \frac{1}{2\pi^{3/2}}\sum_{k=1}^{N^{(\mathrm{H})}}\sum_{l=1}^{N^{(\mathrm{H})}} w_k^{(\mathrm{H})}w_l^{(\mathrm{H})}\exp\left(j\nu 10^{\frac{\sqrt{2}\sigma_{\mathcal{E}}x_l^{(\mathrm{H})}+\mu_{0,0}}{10}}\right) \\ & \exp\left(-\frac{1}{2}\lambda(L-1)T_\mathrm{c}\sum_{p=1}^{N^{(\mathrm{L})}} w_p^{(\mathrm{L})}\left[1-\mathcal{L}_{0,t}(\nu)\right]\right. \\ & \left.\Big|_{t=\frac{1}{2}(L-1)T_\mathrm{c}(x_p^{(\mathrm{L})}+1)}\right) \\ & \exp\left(-\frac{1}{2}\Lambda(L-1)T_\mathrm{c}\sum_{i=1}^{N^{(\mathrm{L})}} w_i^{(\mathrm{L})}\right. \\ & \left.\left[1-\mathcal{L}_{T,T}(\nu)e^{-\lambda\psi_\nu(T)}\right]\Big|_{T=\frac{1}{2}(L-1)T_\mathrm{c}(x_i^{(\mathrm{L})}+1)}\right) \\ & \int_0^\infty Q\left(\sqrt{(1-\rho_r)\frac{E_\mathrm{b}}{N_0}x}\right)\exp(-jx\nu)dx \\ & \exp(\nu^2)\big|_{\nu=x_k^{(\mathrm{H})}}. \end{aligned} \quad (22)$$

IV. Numerical Results

A. Simulation Method

In order to check the correctness of the BER formula in the last section, we perform simulation by MATLAB. We consider the orthogonal binary signal, i.e., the pulse position modulation (PPM) signal. When the information bit is 0, the transmitted signal is

$$s_0(t) = \begin{cases} 1, & 0 \le t < T_\mathrm{c}, \\ 0, & \text{otherwise.} \end{cases} \quad (23)$$

Here we set $T_\mathrm{c} = 1$ nsec. When the information bit is 1, the signal waveform is $s_1(t) = s_0(t - \delta T_\mathrm{c})$, where δ is a positive integer. From the `uwb_sv_model_ct` function in [1], we can get the output vectors $\mathbf{h}$ and $\mathbf{t}$. The vector $\mathbf{t}$ stores the arrival time of every channel impulse response with increasingly chronological order. The vector $\mathbf{h}$ stores the corresponding amplitude.

We define a template vector $\mathbf{p}_0$ with size $1\times(L+\delta)$, where the m-th element of $\mathbf{p}_0$ (denoted by $\mathbf{p}_0[m]$) is equal to

$$\mathbf{p}_0[m] = \begin{cases} \sum_{n:\mathbf{t}[n]=0}\mathbf{h}[n], & m=1, \\ \sum_{n:(m-2)T_\mathrm{c}<\mathbf{t}[n]\le(m-1)T_\mathrm{c}}\mathbf{h}[n], & 2\le m\le L, \\ 0, & L<m\le L+\delta. \end{cases} \quad (24)$$

The physical meaning of vector $\mathbf{p}_0$ is the received signal excluding the noise sampled at a rate of $1/T_\mathrm{c}$ for the information bit 0. If the information bit is 1, then the template vector can be expressed as

$$\mathbf{p}_1 = [\mathbf{0}_{1\times\delta}, \mathbf{p}_0[1], \cdots, \mathbf{p}_0[L]] \quad (25)$$

After adding noise $\mathbf{n}$, the sampled received signal for information bit 0 becomes

$$\mathbf{r} = \mathbf{p}_0 + [\mathbf{n}, \mathbf{0}_{1\times\delta}], \quad (26)$$

and that for information bit 1 is

$$\mathbf{r} = \mathbf{p}_1 + [\mathbf{0}_{1\times\delta}, \mathbf{n}]. \quad (27)$$

Note that the noise vector $\mathbf{n}$ contains L independent identically distributed normal random variables, each of which has zero mean and variance of $N_0/2$.

The coherent RAKE receiver is applied to detect the signal in the IEEE 802.15.3a UWB channel. Let the decision variable $U_0 = \mathbf{r}\cdot\mathbf{p}_0$ and $U_1 = \mathbf{r}\cdot\mathbf{p}_1$, where the operator "$\cdot$" is the inner product of two vectors. If $U_0 \ge U_1$, then the information bit is 0; otherwise, the information bit is 1.

B. Results

Figure 1 shows the PDF $f_{\mathcal{E}}(x)$ for CM1, CM2, CM3, and CM4 according to (21). The number of fingers of the RAKE receiver is 10. CM1 has most probability mass in the high energy range; CM2 ranks second; CM3 ranks third; and CM4 has least probability mass in the range of higher energy range. This phenomenon can explain why CM1 has the best BER performance compared to CM2, CM3, and CM4.

Figure 2 shows the PDF $f_{\mathcal{E}}(x)$ for various numbers of RAKE fingers $L = 20, 30, 40$, and 50 in the channel model CM1. The PDFs of $L = 30, 40$, and 50 are about the same, while the probability mass of $L = 20$ is in the lower energy range.

Figure 3 compares the BER performance based on (7) in [6] and (22) in our paper. For the BER curve based on [6], we reproduce the curve in [6, Fig. 1], where the received waveform is observed only over a finite window $[0, T_{\max}]$ with $T_{\max} = 33$ nsec. The symbol $\eta = \mathcal{E}_\mathrm{w}/(8\sigma_\mathrm{n}^2)$, where $\mathcal{E}_\mathrm{w}$ is the signal energy and σ_n^2 is the noise power spectral density. In the figure, we observe that the BER obtained from (22) is slightly higher than that obtained from (7) of [6] because of the lognormal shadowing.

Figure 4 shows the BER v.s. E_b/N_0 for CM1, CM2, CM3, and CM4 by simulation and analysis for $\rho_r = 0$, i.e., the orthogonal binary signal. The parameter δ of the PPM is set to one, the number of the fingers of the RAKE receiver is 10, and T_c is 1 nsec. For a given E_b/N_0, we simulate 100,000 bits to obtain the BER. As seen from the figure, the analytical

results match the simulation results quite well. However, there are some differences between the simulation and the analytical curves for CM3 and CM4. We explain reasons as follows:

1) The usage of Gauss-Hermite and Gauss-Legendre formulas may cause some error in integrations.
2) We use the MATLAB programs provided in [1] to generate the IEEE 802.15.3a channel. Theoretically, the Poisson process has infinite arrivals, but the computer simulation can only generate finite arrivals. The MATLAB program in [1] only produces the clusters with the arrival time up to 10Γ. Meanwhile, each cluster only contains the rays with the arrival time up to 10γ. Thus, the RAKE receiver in the simulation may collect less energy than that in the ideal case. Thus the simulation BER values are slightly higher than the theoretical BER values.

Figure 5 shows the BER v.s. the number of fingers of the RAKE receiver for CM1, CM2, CM3, and CM4 at $E_{\rm b}/N_0 = 5$ dB. The other parameters are the same as those of the simulation in Fig. 4. As L increases, the BER decreases because of collecting more energy. For a large value of L, the BER curves become flat because the RAKE receiver almost captures all the channel energy. In the figure we can see that the BERs of CM1, CM2, and CM3 converge to a common value when $L = 50$ except for CM4. Note that CM4 has the largest delay spread. Thus, a portion of the energy in the region of $L > 50$ is not received, thereby resulting in higher BER than CM1, CM2, and CM3.

V. Conclusions

In this work, we have derived the BER analytical formula for the antipodal and orthogonal binary signals with a coherent RAKE receiver in the IEEE 802.15.3a UWB channel model. Our numerical results show that the simulation and the analytical values of the BER are very close. The analytical BER formula can significantly save computer simulation time. Furthermore, the suggested analytical method can be applied to other multipath channel models with random numbers of clusters and rays.

The possible future works that can be extended from this work include the following. First, we plan to analyze the same problem under the IEEE 802.15.4a UWB channel model [13]. Second, we are going to find the ergodic capacity of such a UWB channel models.

Appendix I
Proof of Theorem 1

Let $f_{G|T,t}(x)$ be the PDF of the path gain $G \triangleq \alpha_{k,l}$ arriving at time t that is part of a cluster that started at time T. According to [11], $f_{G|T,t}(x)$ can be written as

$$f_{G|T,t}(x) = \frac{1}{2}[f_{|G||T,t}(x) + f_{|G||T,t}(-x)], \qquad (28)$$

because the path gain is positive or negative with equal probability of 0.5. [Recall the definition of path gain in (5) and the following context.] Note that $f_{|G||T,t}(x)$ is lognormally distributed, i.e.,

$$f_{|G||T,t}(x) = \begin{cases} \frac{20\exp\left[-\frac{1}{2\sigma^2}(20\log_{10}x-\mu_{T,t})^2\right]}{\sqrt{2\pi}\sigma x\ln 10}, & x>0, \\ 0, & \text{otherwise.} \end{cases} \qquad (29)$$

where $\mu_{T,t}$ is given in (15) and

$$\sigma = \sqrt{\sigma_1^2 + \sigma_2^2} \qquad (30)$$

are the mean and variance of the random variable $20\log_{10}|G|$, respectively. Note that (15) is the continuous-time representation of (8) because the discrete indices k and l are changed to continuous arrival time t and T, respectively.

The complete form of the square path gain should be X^2G^2, where X is the lognormal shadowing introduced in Section II. Since $20\log_{10}X \propto \text{Normal}(0,\sigma_x^2)$, we have

$$20\log_{10}X^2 = 2(20\log_{10}X) \propto \text{Normal}(0,(2\sigma_x)^2) \ . \qquad (31)$$

Then, it follows that

$$\begin{aligned} 20\log_{10}X^2G^2 &= 2(20\log_{10}X|G|) \\ &= 2(20\log_{10}X) + 2(20\log_{10}|G|) \\ &\propto \text{Normal}(0,(2\sigma_x)^2) + \text{Normal}(2\mu_{T,t},(2\sigma)^2) \\ &\propto \text{Normal}(2\mu_{T,t}, 4(\sigma_1^2+\sigma_2^2+\sigma_x^2)) \ . \end{aligned} \qquad (32)$$

Define $\sigma_{\mathcal{E}} = \sqrt{\sigma_1^2+\sigma_2^2+\sigma_x^2}$. Then the PDF of the square of the path gain arriving at time t in a cluster starting at time T can be written as

$$f_{T,t}(x) = \begin{cases} \frac{10\exp\ -\frac{1}{8\sigma_{\mathcal{E}}^2}(20\log_{10}x-2\mu_{T,t})^2}{\sqrt{2\pi}\sigma_{\mathcal{E}}x\ln 10}, & x>0, \\ 0, & \text{otherwise.} \end{cases} \qquad (33)$$

Denote $\mathcal{L}_{T,t}(\nu)$ as the characteristic function of $f_{T,t}(x)$, i.e.,

$$\mathcal{L}_{T,t}(\nu) = \mathbb{E}_{T,t}[e^{j\nu X^2G^2}] = \int_{-\infty}^{\infty} e^{j\nu x} f_{T,t}(x)dx. \qquad (34)$$

Let $y = \frac{1}{2\sqrt{2}\sigma_{\mathcal{E}}}(20\log_{10}x - 2\mu_{T,t})$ in (14). Then we can have

$$\begin{aligned} &\mathcal{L}_{T,t}(\nu) \\ =\ & \int_{-\infty}^{\infty} \exp\left(j\nu 10^{\frac{2\sqrt{2}\sigma_{\mathcal{E}}y+2\mu_{T,t}}{20}}\right) \frac{10e^{-y^2}}{\sqrt{2\pi}\sigma_{\mathcal{E}}x\ln 10}\frac{x\sigma_{\mathcal{E}}\ln 10}{5\sqrt{2}}dy \\ =\ & \int_{-\infty}^{\infty} \frac{1}{\sqrt{\pi}} \exp\left(j\nu 10^{\frac{\sqrt{2}\sigma_{\mathcal{E}}y+\mu_{T,t}}{10}}\right) e^{-y^2}dy \\ \approx\ & \sum_{l=1}^{N^{(\rm H)}} w_l^{(\rm H)} \frac{1}{\sqrt{\pi}} \exp\left(j\nu 10^{\frac{\sqrt{2}\sigma_{\mathcal{E}}x_l^{(\rm H)}+\mu_{T,t}}{10}}\right). \end{aligned} \qquad (35)$$

Appendix II
Proof of Theorem 2

In [11] the authors have obtained the characteristic function of the sum of path gains in the time window $[a,b]$ (denoted by Φ), but the lognormal shadowing is not taken into account. Similarly, we apply their results to determine the characteristic function of $\mathcal{E}$. Assume that the RAKE receiver with L fingers is used to collect the channel energy in the time window $[0,(L-1)T_{\rm c}]$, where $T_{\rm c}$ is the chip duration between two fingers.

In [11], the authors defined the following functions:

$$\psi_\nu(T) = \begin{cases} \int_{\max(a,T)}^{b} [1 - \mathcal{L}_{T,t}(\nu)]dt, & T \le b, \\ 0, & T > b, \end{cases} \tag{36}$$

and

$$J(\nu) = \int_0^a [1 - e^{-\lambda\psi_\nu(T)}]dT + \int_a^b [1 - \mathcal{L}_{T,T}(\nu)e^{-\lambda\psi_\nu(T)}]dT. \tag{37}$$

We set $a = 0$, $b = (L-1)T_{\mathrm{c}}$ and use the Gauss-Legendre formula. Then we can transform the above equations to (18) and (20), respectively.

REFERENCES

[1] J. Foerster, et. al., "Channel modeling sub-committee report final," *IEEE P802.15 Wireless Personal Area Networks, P802.15-02/490r1-SG3a*, Feb. 2003.

[2] K. Eshima, Y. Hase, S. Oomori, F. Takahashi, and R. Kohno, "M-ary UWB system using Walsh codes," *IEEE Conference on Ultra Wideband Systems and Technologies*, pp. 37–40, May 21–23, 2002.

[3] M. Hämäläinen, R. Tesi, and J. Iinatti, "On the UWB system performance studies in AWGN channel with interference in UMTS band," *IEEE Conference on Ultra Wideband Systems and Technologies*, pp. 321–325, May 21–23, 2002.

[4] İ. Güvenç and H. Arslan, "Performance evaluation of UWB systems in the presence of timing jitter," *IEEE Conference on Ultra Wideband Systems and Technologies*, pp. 136–141, Nov. 16–19, 2003.

[5] T. Q. S. Quek and M. Z. Win, "Ultrawide bandwidth transmitted-reference signaling," *IEEE International Conference on Communications*, vol. 6, pp. 3409–3413, June 20–24, 2004.

[6] J. A. Gubner and K. Hao, "A computable formula for the average bit-error probability as a function of window size for the IEEE 802.15.3a UWB channel model," *IEEE Trans. Microwave Theory Tech.*, submitted for publication. [Online]. Available: http://homepages.cae.wisc.edu/~gubner/GubnerHao_MTT_UWB.pdf

[7] K. Hao and J. A. Gubner, "Performance measures and statistical quantities of rake receivers using maximal-ratio combining on the IEEE 802.15.3a UWB channel model," *IEEE Trans. Wireless Commun.*, submitted for publication. [Online]. Available: http://homepages.cae.wisc.edu/~gubner/HaoGubnerTWaf2col.pdf

[8] L.-C. Wang, W.-C. Liu, and K.-J. Shieh, "On the performance of using multiple transmit and receive antennas in pulse-based ultrawideband systems," *IEEE Trans. Wireless Commun.*, vol. 4, no. 6, pp. 2738–2750, Nov. 2005.

[9] H. Liu, R. C. Qiu, and Z. Tian, "Error performance of pulse-based ultra-wideband MIMO systems over indoor wireless channels," *IEEE Trans. Wireless Commun.*, vol. 4, no. 6, pp. 2939–2944, Nov. 2005.

[10] J. G. Proakis, *Digital Communications*, 4th ed. Boston: McGraw-Hill, 2001.

[11] K. Hao and J. A. Gubner, "The distribution of sums of path gains in the IEEE 802.15.3a UWB channel model," *IEEE Trans. Wireless Commun.*, submitted for publication. [Online]. Available: http://homepages.cae.wisc.edu/~gubner/HaoGubnerTWireless2col.pdf

[12] [Online]. Available: http://www.efunda.com/math/num_integration/num_int_gauss.cfm

[13] A. F. Molisch et al., "IEEE 802.15.4a channel model - final report," IEEE 802.15 WPAN Low Rate Alternative PHY Task Group 4a (TG4a), Tech. Rep., Nov. 2004.

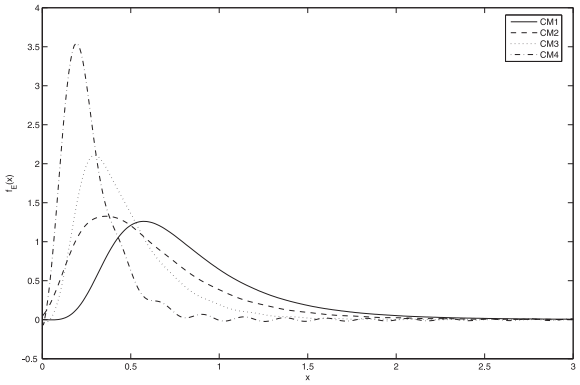

Fig. 1. The PDF $f_{\mathcal{E}}(x)$ for a RAKE receiver with 10 fingers in the IEEE 802.15.3a UWB channels CM1, CM2, CM3, and CM4.

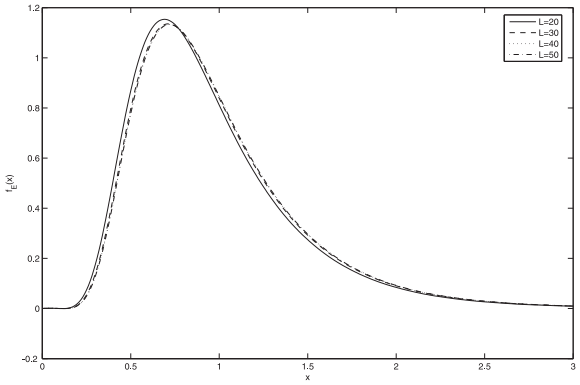

Fig. 2. The PDF $f_{\mathcal{E}}(x)$ of a RAKE receiver with finger number $L = 20, 30, 40$, and 50 in the IEEE 802.15.3a UWB channel CM1.

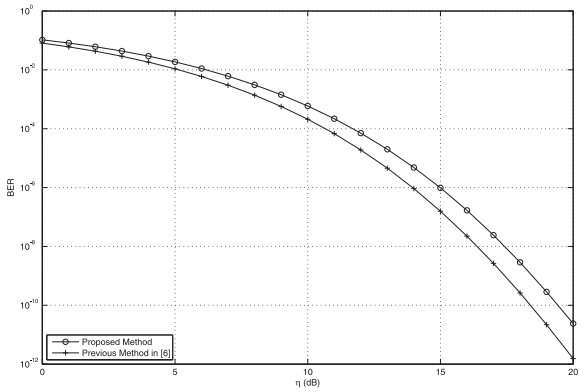

Fig. 3. BER comparison of the proposed analytical formulas with that in [6], where $T_{\max} = 33$ nsec.

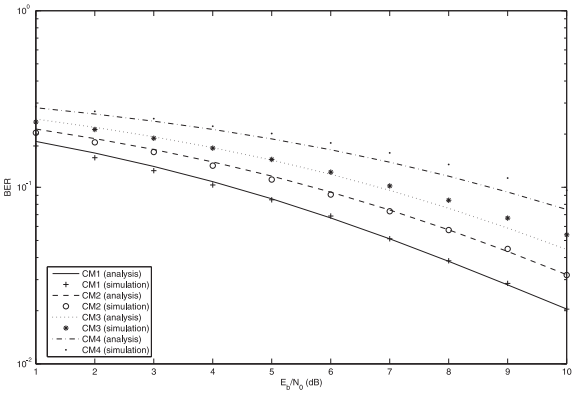

Fig. 4. The BER v.s. $E_{\rm b}/N_0$ for the RAKE receiver with 10 fingers in the IEEE 802.15.3a UWB channels CM1, CM2, CM3, and CM4.

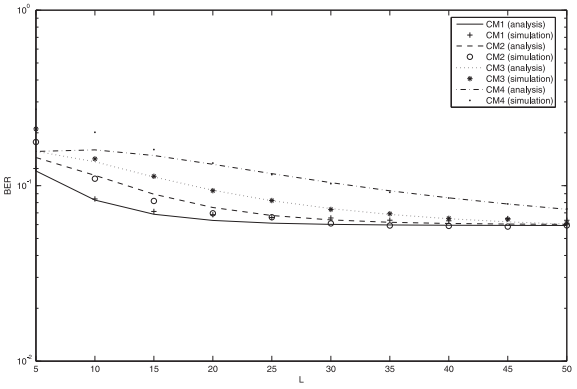

Fig. 5. The BER v.s. the number of fingers of the RAKE receiver (L) for CM1, CM2, CM3, and CM4, where $E_{\rm b}/N_0 = 5$ dB.

BER Analysis of the IEEE 802.15.4a Channel Model with RAKE Receiver

Wei-Cheng Liu and Li-Chun Wang
Department of Communication Engineering
National Chiao Tung University, Hsinchu, Taiwan
lichun@cc.nctu.edu.tw, Tel: +886-3-5712121 ext 54511

***Abstract*— This paper provides the bit error rate (BER) analysis of the antipodal and orthogonal binary signals under the ultra-wideband (UWB) channel. We offer an analytical expression and its evaluation formula for the BER. The channel model we consider is the IEEE 802.15.4a UWB channel. We take into account of the impact of all the key parameters, including inter-cluster arrival rate, cluster decay constant, the inter-ray arrival rate, ray decay constant, parameters of the power delay profile (PDP), and the distribution of a Nakagami fading signal. For the IEEE 802.15.4a UWB channel, the effects of clustering are characterized by a Poisson process, and the inter-ray arrival time is modeled as the hyperexponential random variable. We propose a systematic analytical method to evaluate the BER performance of the UWB signal associated with such joint continuous Nakagami and discrete Poisson random variable. Thus, the developed analytical model is useful in evaluating the performance of an UWB signal in the IEEE 802.15.4a channel without time consuming simulations.**

***Index Terms*— Ultra-wideband (UWB), IEEE 802.15.4a channel model, bit error rate (BER).**

I. Introduction

THE trend of the modern wireless systems is to achieve higher data rates and better quality. The ultra-wideband (UWB) communications is a possible technique to achieve this objective, due to its extremely large bandwidth. Performance analysis, such as bit error rate (BER) analysis, of the UWB communication system in a *realistic* UWB channel is important but a difficult task.

In this work, we use the IEEE 802.15.4a UWB channel model [1] as our channel model, which is based on the recent measurements and close to the realistic UWB channel. The UWB channel has two important properties that is different from the traditional narrow band channel: 1) The bandwidth of the UWB signals is much larger than the coherence bandwidth of the channel. Thus, in the frequency domain, the severely highly frequency selective fading occurs. 2) The large bandwidth results in high resolution arrival time for the UWB signal. Thus, the reflected UWB waves by objects arrive in many clusters, which may contain some non-Rayleigh multipath components.

A. Motivation

The difficulties of analyzing UWB signals can be discussed in three aspects.

[1]This work is supported by the National Science Council, Taiwan, under the contract NSC94-2213-E-009-030.

- First, the narrow band channel model does not have the concept of cluster. The number of the channel impulse response is a fixed constant. On the contrary, the transmitted signal over the UWB channel may arrive in many clusters, of which the number of arrival rays is random. The number of the clusters is also random, which is modeled as the Poisson random variable. Mathematically, the interarrival time of the rays within a cluster is the hyperexponential random variable. The collected signal energy at the RAKE receiver in a channel with random number of clusters and rays is difficult to analyze.
- The amplitude of the impulse response in the UWB channel is a multidimensional random variable, consisting of the Nakagami m faded amplitude with a mean related to an exponential and a hyperexponential random variable. This is because the average of the channel impulse is also a random variable due to varying interarrival time of rays and clusters. The parameter m of the Nakagami random variable is a lognormal random variable, of which the mean and the standard deviation are both dependent on the arrival time of the rays.
- The number of arrival rays in a very narrow time bin (or chip duration) is not very large, so the central limit theorem is no longer applicable here. Thus, the distribution of fading is not a traditional Rayleigh random variable as in the narrow band case. In the IEEE 802.15.4a UWB channel, the multipath fading signal is characterized by a Nakagami m random variable according to measurement results. Thus, for a given number of rays and the mean of the signal amplitude, a UWB signal is a fast-varying Nakagami m faded random variable. The analysis of such a signal is rarely seen in current literature.

The IEEE 802.15.4a UWB channel model defines nine sets of parameters for different environments. Based on this channel model, a UWB signal can be characterized by a joint continuous Nakagami m, a discrete Poisson random variable for clusters, and a discrete counting random variable with interarrival time being hyperexponential distributed, of which key parameters include the inter-cluster arrival rate, ray arrival rates (mixed Poisson model parameters), inter-cluster decay constant, intra-cluster decay time constant parameters, Nakagami m factor mean, Nakagami m factor variance, Nakagami m factor for strong components, and parameters for alternative power delay profile (PDP) shape.

To our best knowledge, a complete analytical formula for the bit error rate (BER) performance with RAKE receiver in the IEEE 802.15.4a UWB channel considering all the three aforementioned challenges and key parameters is not seen in the literature. Even only the analysis of the IEEE 802.15.4a UWB channel model is an open issue.

B. Related Work

In this subsection, we introduce some related works which has the correlation to the performance analysis of the UWB system under different channels. In [2], the authors derived the analytical BER of binary and M-ary UWB systems with Walsh codes under the AWGN channel with multiple access interference (MAI). In [3], the authors studied the performances of UWB systems in the AWGN channel with interference in the universal mobile telecommunications system (UMTS)/wideband code division multiple access (WCDMA) band. In [4], the authors derived the BER formula of the UWB system under the flat and dispersive Rayleigh fading channels with timing jitter. In [5], the authors analyzed the performance of a transmit-reference (TR) UWB system with an autocorrelation receiver under a slow fading channel of which fading amplitude is characterized by an appropriate moment generating function.

In [6], the authors derived a exact BER formula for the IEEE 802.15.3a UWB channel model [7] but only as a function of finite window size rather than a function of the fingers number of the RAKE receiver. In [8], they further obtained statistics of the output signal-to-noise ratio (SNR) for the RAKE receiver in the IEEE 802.15.3a UWB channel, but without providing explicit BER formula and ignored the shadowing effect. In [9], the authors have derived the BER analytical formula for receiving the antipodal and orthogonal binary signals by using a coherent RAKE receiver over the *complete* IEEE 802.15.3a UWB channel model.

Reference [10] presented an analytical expression for the SNR of the pulse position modulated (PPM) signal in a multi input multi output (MIMO) UWB channel. The considered UWB channel has the following three major properties: 1) Gamma distribution to describe each resolvable path power; 2) a modified Poisson process to characterize the clustering property of the UWB channel and the number of the simultaneous arrival paths; 3) exponential decay to model the average resolvable path power in the time domain. In [11], the theoretical error performance of a zero-forcing (ZF) RAKE receiver system over the frequency-selective UWB lognormal fading channels with MIMO was analyzed.

C. Objective and Outline of This Paper

The objective of this paper is to derive the analytical BER expression for the UWB system using the coherent RAKE receiver in a complete IEEE 802.15.4a UWB channel. Furthermore, we obtain a practical evaluation equation to compute the BER much more quickly, compared to do computer simulation. The rest of this paper is organized as follows. In Section II, we describe the IEEE 802.15.4a channel model. In Section III, we derive the evaluation form expression for BER of the antipodal and orthogonal binary signals under the IEEE 802.15.4a UWB channel. In Section IV, we show our numerical results. Last, we give our conclusions in Section V.

II. Channel Model

A. Power delay profile

We consider the UWB channel model in [1]. The impulse response (in complex baseband) of the Saleh-Valenzuela (SV) model is given in general as

$$h_{discr}(t) = \sum_{l=0}^{L}\sum_{k=0}^{K} a_{k,l}\exp(j\phi_{k,l})\delta(t - T_l - \tau_{k,l}) \qquad (1)$$

where $a_{k,l}$ is the tap weight of the kth component in the lth cluster, T_l is the delay of the lth cluster, $\tau_{k,l}$ is the delay of the kth multipath component (MPC) relative to the l-th cluster arrival time T_l. The phases $\phi_{k,l}$ are uniformly distributed, i.e., for a bandpass system, the phase is taken as a uniformly distributed random variable from the range $[0, 2\pi]$. The number of clusters L is an important parameter of the model. It is assumed to be Poisson-distributed

$$f_L(L) = \frac{(\overline{L})^L \exp(-\overline{L})}{L!} \qquad (2)$$

so that the mean $\overline{L}$ completely characterizes the distribution.

By definition, we have $\tau_{0,l} = 0$. The distributions of the cluster arrival times are given by a Poisson processes

$$p(T_l|T_{l-1}) = \begin{cases} \Lambda_l \exp[-\Lambda(T_l - T_{l-1})], & T_l > T_{l-1} \\ 0, & \text{otherwise} \end{cases}, l > 0 \qquad (3)$$

where Λ_l is the cluster arrival rate (assumed to be independent of l). The classical SV model also uses a Poisson process for the ray arrival times. Due to the discrepancy in the fitting for the indoor residential, and indoor and outdoor office environments, the authors of [1] propose to model ray arrival times with mixtures of two Poisson processes as follows

$$\begin{aligned} & p(\tau_{k,l}|\tau_{(k-1),l}) \\ = & \begin{cases} \beta\lambda_1 \exp[-\lambda_1(\tau_{k,l} - \tau_{(k-1),l})] + \\ (1-\beta)\lambda_2 \exp[-\lambda_2(\tau_{k,l} - \tau_{(k-1),l})], & \tau_{k,l} > \tau_{(k-1),l} \\ 0, & \text{otherwise} \end{cases}, \\ & k > 0, \end{aligned} \qquad (4)$$

where β is the mixture probability, while λ_1 and λ_2 are the ray arrival rates.

The next step is the determination of the cluster powers and cluster shapes. The power delay profile (mean power of the different paths) is exponential within each cluster

$$E\{|a_{k,l}|^2\} = \frac{\Omega_l}{\gamma_l}\exp(-\tau_{k,l}/\gamma_l) \qquad (5)$$

where Ω_l is the integrated energy of the lth cluster, and γ_l is the intra-cluster decay time constant. Note that the normalization is an approximate one, but works for typical values of λ and γ.

The cluster decay rates are found to depend linearly on the arrival time of the cluster,

$$\gamma_l \propto k_\gamma T_l + \gamma_0 \qquad (6)$$

where k_γ describes the increase of the decay constant with delay.

The mean (over the cluster shadowing) mean (over the small-scale fading) energy (normalized to γ_l), of the lth cluster follows in general an exponential decay

$$10\log(\Omega_l) = 10\log(\exp(-T_l/\Gamma)) + M_{cluster} \tag{7}$$

where $M_{cluster}$ is a normally distributed variable with standard deviation $\sigma_{cluster}$ around it.

For the non-line-of-sight (NLOS) case of some environments (office and industrial), the shape of the power delay profile can be different, namely (on a log-linear scale)

$$\begin{aligned} E\{|a_{k,1}|^2\} &= (1-\chi\exp(-\tau_{k,l}/\gamma_{\text{rise}}))\exp(-\tau_{k,l}/\gamma_1) \\ &\quad \frac{\gamma_1+\gamma_{\text{rise}}}{\gamma_1}\frac{\Omega_1}{\gamma_1+\gamma_{\text{rise}}(1-\chi)}. \end{aligned} \tag{8}$$

Here, the parameter χ describes the attenuation of the first component, the parameter γ_{rise} determines how fast the PDP increases to its local maximum, and γ_1 determines the decay at late times.

B. Small-scale fading

The distribution of the small-scale amplitudes is Nakagami

$$f_a(x) = \frac{2}{\Gamma(m)}\left(\frac{m}{\Omega}\right)^m x^{2m-1}\exp\left(-\frac{m}{\Omega}x^2\right), \tag{9}$$

where $m \geq 1/2$ is the Nakagami m-factor, $\Gamma(m)$ is the gamma function, and Ω is the mean-square value of the amplitude. A conversion to a Rice distribution is approximately possible with the conversion equations

$$m = \frac{(K_{\text{r}}+1)^2}{(2K_{\text{r}}+1)} \tag{10}$$

and

$$K_{\text{r}} = \frac{\sqrt{m^2-m}}{m-\sqrt{m^2-m}}. \tag{11}$$

where K_{r} and m are the Rice factor and Nakagami-m factor respectively.

The parameter Ω corresponds to the mean power, and its delay dependence is thus given by the power delay profile above. The m–parameter is modeled as a lognormally distributed random variable, whose logarithm has a mean μ_{m} and standard deviation σ_{m}. Both of these can have a delay dependence

$$\mu_{\text{m}}(\tau) = m_0 - k_{\text{m}}\tau \tag{12}$$

$$\sigma_{\text{m}}(\tau) = \widehat{m}_0 - \widehat{k}_{\text{m}}\tau \tag{13}$$

For the first component of each cluster, the Nakagami factor is modeled differently. It is assumed to be deterministic and independent of delay $m = \widetilde{m}_0$.

III. BER Analysis

A. Receiver Structure

We use a coherent RAKE receiver with L_{RAKE} fingers. The received SNR γ_{b} is

$$\gamma_{\text{b}} = \frac{E_{\text{b}}}{N_0}\sum_{k=1}^{L} c_k^2, \tag{14}$$

where E_{b}/N_0 is the bit SNR, c_k is the channel amplitude that appears at the k-th finger of the RAKE receiver. From [12] we know that the conditional error probability for binary signals for the coherent RAKE receiver is

$$P_2(\gamma_{\text{b}}) = Q\left(\sqrt{\gamma_{\text{b}}(1-\rho_r)}\right) \tag{15}$$

where $\rho_r = -1$ for antipodal signals and $\rho_r = 0$ for orthogonal signals. Next we will derive the characteristic function of the received energy $\mathcal{E} \triangleq \sum_{k=1}^{L} c_k^2$ in the IEEE 802.15.4a UWB channel.

B. Characteristic Function of the Received Energy ($\mathcal{E}$)

In the following theorem, we give the formula of the characteristic function of $\mathcal{E}$. We exploit the result in [9] and modify it to fit in the case of the IEEE 802.15.4a UWB channel.

Lemma 1: Let $\mathcal{L}_{T,t}(\nu)$ be the characteristic function of the squared single path gain in the IEEE 802.15.4a UWB channel with the cluster arrival time at T and the ray arrival time at $t = T+\tau$. Also, denote $e^{-\lambda\psi_\nu(T)}$ and $e^{-\Lambda J(\nu)}$ the characteristic function of a shot-noise random variable related to the ray arrival process with parameter λ and that related to the cluster arrival process with parameter Λ, respectively. Then, it can be proved that the characteristic function of the received energy ($\mathcal{E}$) in the IEEE 802.15.4a UWB channel can be computed by

$$\Psi(\nu) = \mathcal{L}_{0,0}(\nu)e^{-\lambda\psi_\nu(0)-\Lambda J(\nu)}. \tag{16}$$

Proof: See [9]. ■

Theorem 1: Consider a RAKE receiver with L_{RAKE} fingers in the IEEE 802.15.4a UWB channel. The characteristic function $\mathcal{L}_{T,t}(\nu)$ can be computed by

$$\mathcal{L}_{T,t}(\nu) = (1-j\nu\Omega/m)^{-m} \tag{17}$$

where

$$\Omega = \frac{1}{\gamma_l}\exp\left(-\frac{T}{\Gamma}-\frac{t-T}{\gamma_l}\right) \tag{18}$$

and

$$m = \exp\left(m_0+\widehat{m}_0^2/2\right). \tag{19}$$

The parameter γ_l is defined in (6).

Proof: See Appendix I. ■

Theorem 2: The parameter λ in Lemma 1 can be calculated as

$$\lambda = \frac{\lambda_1\lambda_2}{(1-\beta)\lambda_1+\beta\lambda_2}. \tag{20}$$

Proof: See Appendix II. ■

The equations for calculating $\psi_\nu(T)$ and $J(\nu)$ can be found in Theorem 2 in [9].

With characteristic function of $\mathcal{E}$, i.e. $\Psi(\nu)$ in (16), the probability density function (PDF) of $\mathcal{E}$ can be computed by the Gauss-Hermite formula as follows:

$$\begin{aligned} f_{\mathcal{E}}(x) &= \frac{1}{2\pi}\int_{-\infty}^{\infty}\Psi(\nu)e^{-jx\nu}d\nu \\ &\approx \frac{1}{2\pi}\sum_{k=1}^{N^{(\mathrm{H})}} w_k^{(\mathrm{H})}\Psi(\nu)e^{-jx\nu}e^{\nu^2}\Big|_{\nu=x_k^{(\mathrm{H})}}. \end{aligned} \quad (21)$$

Combining (17), (21), and (16) and (17) in [9], the BER of the RAKE receiver in the IEEE 802.15.4a UWB channel can be computed as

$$\begin{aligned} P_2 &= \mathbb{E}_{\mathcal{E}}\left[Q\left(\sqrt{(1-\rho_r)\frac{E_\mathrm{b}}{N_0}\mathcal{E}}\right)\right] \\ &= \int_0^\infty Q\left(\sqrt{(1-\rho_r)\frac{E_\mathrm{b}}{N_0}x}\right)f_{\mathcal{E}}(x)dx \\ &= \frac{1}{2\pi}\left(1-j\frac{\nu}{\gamma_0\exp\left(m_0+\widehat{m}_0^2/2\right)}\right)^{-\exp\left(m_0+\widehat{m}_0^2/2\right)} \\ &\quad \sum_{k=1}^{N^{(\mathrm{H})}} w_k^{(\mathrm{H})}\exp\left(-\frac{1}{2}\lambda(L-1)T_\mathrm{c}\sum_{p=1}^{N^{(\mathrm{L})}} w_p^{(\mathrm{L})}\right. \\ &\quad \left.[1-\mathcal{L}_{0,t}(\nu)]\big|_{t=\frac{1}{2}(L-1)T_\mathrm{c}(x_p^{(\mathrm{L})}+1)}\right) \\ &\quad \exp\left(-\frac{1}{2}\Lambda(L-1)T_\mathrm{c}\sum_{i=1}^{N^{(\mathrm{L})}} w_i^{(\mathrm{L})}\right. \\ &\quad \left.\left[1-\mathcal{L}_{T,T}(\nu)e^{-\lambda\psi_\nu(T)}\right]\Big|_{T=\frac{1}{2}(L-1)T_\mathrm{c}(x_i^{(\mathrm{L})}+1)}\right) \\ &\quad \int_0^\infty Q\left(\sqrt{(1-\rho_r)\frac{E_\mathrm{b}}{N_0}x}\right)\exp(-jx\nu)dx \\ &\quad \exp(\nu^2)\big|_{\nu=x_k^{(\mathrm{H})}}. \end{aligned} \quad (22)$$

IV. Numerical Results

A. Simulation Method

In order to check the correctness of the BER formula in the last section, we perform simulation by using MATLAB. We consider the orthogonal binary signal, i.e. the PPM signal. When the information bit is 0, the transmitted signal is

$$s_0(t) = \begin{cases} 1, & 0 \le t < T_\mathrm{c}, \\ 0, & \text{otherwise.} \end{cases} \quad (23)$$

Here we set $T_\mathrm{c} = 1$ nsec. When the information bit is 1, the signal waveform is $s_1(t) = s_0(t - \delta T_\mathrm{c})$, where δ is a positive integer. From the `uwb_sv_model_ct_15_4a.m` function in [1], we can get the output vectors $\mathbf{h}$ and $\mathbf{t}$. The vector $\mathbf{t}$ stores the arrival time of every channel impulse response with increasing chronological order. The vector $\mathbf{h}$ stores the corresponding amplitude.

We define a template vector $\mathbf{p}_0$ with size $1 \times (L_{\mathrm{RAKE}} + \delta)$, where the m-th element of $\mathbf{p}_0$ (denote by $\mathbf{p}_0[m]$) is equal to

$$\mathbf{p}_0[m] = \begin{cases} \sum_{n:\mathbf{t}[n]=0}\mathbf{h}[n], & m = 1, \\ \sum_{n:(m-2)T_\mathrm{c}<\mathbf{t}[n]\le(m-1)T_\mathrm{c}}\mathbf{h}[n], & 2 \le m \le L_{\mathrm{RAKE}}, \\ 0, & L_{\mathrm{RAKE}} < m \le \\ & L_{\mathrm{RAKE}} + \delta. \end{cases} \quad (24)$$

The physical meaning of the vector $\mathbf{p}_0$ is the received signal excluding the noise sampled at a rate of $1/T_\mathrm{c}$ given the information bit being 0. If the information bit is 1, then the template vector can be expressed as

$$\mathbf{p}_1[m] = [\mathbf{0}_{1\times\delta}, \mathbf{p}_0[1], \cdots, \mathbf{p}_0[L_{\mathrm{RAKE}}]] \quad (25)$$

After adding noise $\mathbf{n}$, the sampled received signal for information bit 0 becomes

$$\mathbf{r} = \mathbf{p}_0 + [\mathbf{n}, \mathbf{0}_{1\times\delta}], \quad (26)$$

and that for information bit 1 is

$$\mathbf{r} = \mathbf{p}_1 + [\mathbf{0}_{1\times\delta}, \mathbf{n}]. \quad (27)$$

Note that the noise vector $\mathbf{n}$ contains L_{RAKE} independent identically distributed complex normal random variables, each of which has zero mean and variance of N_0.

The coherent RAKE receiver is applied to detect the signal in the IEEE 802.15.4a UWB channel. Let the decision variable $U_0 = \Re(\mathbf{r}\cdot\mathbf{p}_0)$ and $U_1 = \Re(\mathbf{r}\cdot\mathbf{p}_1)$, where $\Re(z)$ is the real part of a complex number z and "$\cdot$" is the inner product of two vectors. If $U_0 \ge U_1$, then the information bit is 0, otherwise the information bit is 1.

B. Results

Figure 1 shows the BER v.s. E_b/N_0 for CM1 by simulation and analysis. The term CM1 denotes the residential line-of-sight (LOS) environment. The parameters of CM1 can be found in the Table in [1, Sec. III.A]. For the analytical curves, We consider the orthogonal binary signal, i.e., $\rho_r = 0$. The parameter δ of the PPM is set to be one. The number of the fingers of the RAKE receiver is 10. The space of the fingers of the RAKE receiver, T_c, is set to 1 nsec. For each given E_b/N_0, we simulate 100,000 bits to obtain the BER. As seen from the figure, the analytical results match the simulation results quite well.

V. Conclusions

In this paper, we have derived the BER analytical formula as well as a computable equation for the antipodal and orthogonal binary signals with a coherent RAKE receiver under the IEEE 802.15.4a UWB channel model. Our numerical results show that the simulation and the analytical values of the BER are extremely close. Our proposed analytical BER formula can obtain the BER values much more quickly, compared to to the computer simulation. Furthermore, we would like to emphasis that the suggested analytical method can be applied to other multipath channel models with any fading distribution.

The possible future works that can be extended from this work include the following. First, we plan to analyze the

same problem under the IEEE 802.15.4a UWB channel model plus MIMO system. Second, we are going to find the ergodic capacity of such a UWB channel models. Third, we want to design the whole transmitter and receiver of the UWB MIMO wireless communication systems.

APPENDIX I
PROOF OF THEOREM 1

From (9), we can easily find the PDF of $x = a^2$ by exploiting the resulting of Example 7b in [13]. That is,

$$\begin{aligned} f_x(x) &= \frac{1}{2\sqrt{x}}\left[f_a(\sqrt{x}) + f_a(-\sqrt{x})\right] \\ &= \begin{cases} \frac{\exp\left(-\frac{mx}{\Omega}\right)\left(\frac{mx}{\Omega}\right)^m}{x\Gamma(m)}, & x \geq 0, \\ 0, & x < 0. \end{cases} \end{aligned} \tag{28}$$

The characteristic function of x is

$$\begin{aligned} \mathcal{L}_{T,t}(\nu) &= \int_{\infty}^{\infty} f_x(x) e^{j\nu x} dx \\ &= (1 - j\nu\Omega/m)^{-m}. \end{aligned} \tag{29}$$

The term $\Omega = E\{x\}$ is defined in (5). To fit it into our formula, we substitute T_l by T and $M_{cluster}$ by its mean, zero, in (7) and $\tau_{k,l}$ by $(t - T)$ in (5). Then we can get (18).

Finally, we set m to its mean and get (19). The mean is given by (4) in [14].

APPENDIX II
PROOF OF THEOREM 2

To find the average arrival rate λ, we lend a concept from the queueing theory [15] that

$$\begin{aligned} \lambda &= 1/E[\text{average interarrival time}] \\ &= \left\{\int_0^{\infty} x\left[\beta\lambda_1 e^{-\lambda_1 x} + (1-\beta)\lambda_2 e^{-\lambda_2 x}\right] dx\right\}^{-1} \\ &= \frac{\lambda_1\lambda_2}{(1-\beta)\lambda_1 + \beta\lambda_2}. \end{aligned} \tag{30}$$

REFERENCES

[1] A. F. Molisch et al., "IEEE 802.15.4a channel model - final report," IEEE 802.15 WPAN Low Rate Alternative PHY Task Group 4a (TG4a), Tech. Rep., Nov. 2004.

[2] K. Eshima, Y. Hase, S. Oomori, F. Takahashi, and R. Kohno, "M-ary UWB system using Walsh codes," *IEEE Conference on Ultra Wideband Systems and Technologies*, pp. 37–40, May 21–23, 2002.

[3] M. Hämäläinen, R. Tesi, and J. Iinatti, "On the UWB system performance studies in AWGN channel with interference in UMTS band," *IEEE Conference on Ultra Wideband Systems and Technologies*, pp. 321–325, May 21–23, 2002.

[4] İ. Güvenç and H. Arslan, "Performance evaluation of UWB systems in the presence of timing jitter," *IEEE Conference on Ultra Wideband Systems and Technologies*, pp. 136–141, Nov. 16–19, 2003.

[5] T. Q. S. Quek and M. Z. Win, "Ultrawide bandwidth transmitted-reference signaling," *IEEE International Conference on Communications*, vol. 6, pp. 3409–3413, June 20–24, 2004.

[6] J. A. Gubner and K. Hao, "A computable formula for the average bit-error probability as a function of window size for the IEEE 802.15.3a UWB channel model," *IEEE Trans. Microwave Theory Tech.*, submitted for publication. [Online]. Available: http://homepages.cae.wisc.edu/~gubner/GubnerHao_MTT_UWB.pdf

[7] J. Foerster, et. al., "Channel modeling sub-committee report final," *IEEE P802.15 Wireless Personal Area Networks, P802.15-02/490r1-SG3a*, Feb. 2003.

[8] K. Hao and J. A. Gubner, "Performance measures and statistical quantities of rake receivers using maximal-ratio combining on the IEEE 802.15.3a UWB channel model," *IEEE Trans. Wireless Commun.*, submitted for publication. [Online]. Available: http://homepages.cae.wisc.edu/~gubner/HaoGubnerTWaf2col.pdf

[9] W.-C. Liu and L.-C. Wang, "Performance analysis of pulse based ultra-wideband systems in the highly frequency selective fading channel with cluster property," *IEEE Vehicular Technology Conference*, May 7–10, 2006, to be published.

[10] L.-C. Wang, W.-C. Liu, and K.-J. Shieh, "On the performance of using multiple transmit and receive antennas in pulse-based ultrawideband systems," *IEEE Trans. Wireless Commun.*, vol. 4, no. 6, pp. 2738–2750, Nov. 2005.

[11] H. Liu, R. C. Qiu, and Z. Tian, "Error performance of pulse-based ultra-wideband MIMO systems over indoor wireless channels," *IEEE Trans. Wireless Commun.*, vol. 4, no. 6, pp. 2939–2944, Nov. 2005.

[12] J. G. Proakis, *Digital Communications*, 4th ed. Boston: McGraw-Hill, 2001.

[13] S. Ross, *A First Course in Probability*, 5th ed. Prentice-Hall International, Inc., 1998.

[14] E. W. Weisstein, "Log normal distribution," *MathWorld–A Wolfram Web Resource*. [Online]. Available: http://mathworld.wolfram.com/LogNormalDistribution.html

[15] A. Krendzel, "Arrival and service processes basic definitions of queueing theory," *Teletraffic Theory Part I: Queueing Theory*. [Online]. Available: http://www.cs.tut.fi/kurssit/8303700/exercise2004(3).ppt

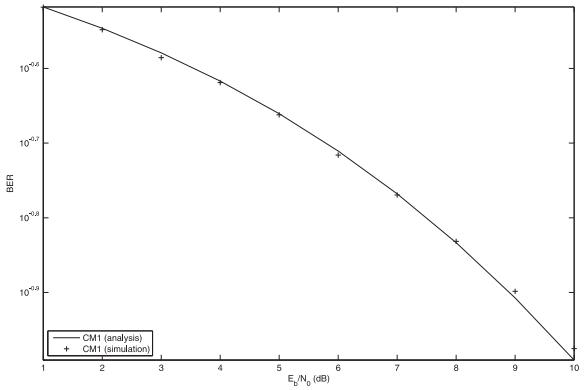

Fig. 1. The BER v.s. $E_{\rm b}/N_0$ for the RAKE receiver with 10 fingers in the IEEE 802.15.4a UWB channel CM1.